Talanta 217 (2020) 121074

Contents lists available at ScienceDirect

Talanta

journal homepage: www.elsevier.com/locate/talanta

Stability of oxylipins during plasma generation and long-term storage

Elisabeth Koch[a,1], Malwina Mainka[a,1], Céline Dalle[b], Annika I. Ostermann[a], Katharina M. Rund[a], Laura Kutzner[a], Laura-Fabienne Froehlich[a], Justine Bertrand-Michel[c], Cécile Gladine[b], Nils Helge Schebb[a,*]

[a] Chair of Food Chemistry, Faculty of Mathematics and Natural Sciences, University of Wuppertal, Wuppertal, Germany
[b] Université Clermont Auvergne, INRAe, UNH, Clermont-Ferrand, France
[c] MetaToul-MetaboHUB, Inserm/UPS UMR 1048 - I2MC, Institut des Maladies Métaboliques et Cardiovasculaires, Toulouse, France

ARTICLE INFO

Keywords:
Eicosanoids
Lipid mediators
LC-MS/MS
Blood sampling

ABSTRACT

Oxidized unsaturated fatty acids – i.e. eicosanoids and other oxylipins – are lipid mediators involved in the regulation of numerous physiological functions such as inflammation, blood coagulation, vascular tone and endothelial permeability. They have raised strong interest in clinical lipidomics in order to understand their role in health and diseases and their use as biomarkers. However, before the clinical translation, it is crucial to validate the analytical reliability of oxylipins. This notably requires to assess the putative artificial formation or degradation of oxylipins by (unsuitable) blood handling during plasma generation, storage and sample preparation. Using a liquid chromatography-mass spectrometry method covering 133 oxylipins we comprehensively analyzed the total (free + esterified) oxylipin profile in plasma and investigated the influence of i) addition of additives during sample preparation, ii) different storage times and temperatures during the transitory stage of plasma generation and iii) long-term storage of plasma samples at −80 °C. Addition of radical scavenger butylated hydroxytoluene reduced the apparent concentrations of hydroxy-PUFA and thus should be added to the samples at the beginning of sample preparation. The concentrations of all oxylipin classes remained stable (within analytical variance of 20%) during the transitory stage of plasma generation up to 24 h at 4 °C or 4 h at 20 °C before centrifugation of EDTA-whole blood and up to 5 days at −20 °C after plasma separation. The variations in oxylipin concentrations did not correlate with storage time, storage temperature or stage of plasma generation. A significant increase of potentially lipoxygenase derived hydroxy-PUFA compared to immediate processing was only detected when samples were stored for longer times before centrifugation, plasma separation as well as freezing of plasma revealing residual enzymatic activity. Autoxidative rather than enzymatic processes led to a slightly increased concentration of 9-HETE when plasma samples were stored at −80 °C for 15 months. Overall, we demonstrate that total plasma oxylipins are robust regarding delays during plasma generation and long-term storage at −80 °C supporting the application of oxylipin profiling in clinical research.

1. Introduction

Eicosanoids and other oxylipins are oxygenated metabolites of polyunsaturated fatty acids (PUFA) which are formed via three different enzymatic pathways and autoxidation [1–3]. These pathways result in a diversity of products from different PUFA, e.g. cyclooxygenase (COX) conversion leads to prostanoids such as prostaglandins and thromboxanes [4], lipoxygenase (LOX) conversion leads via hydroperoxy-PUFA to mid-chain hydroxy- or multiple hydroxylated-PUFA [5] and conversion by cytochrome P450 monooxygenases (CYP) leads either to terminal (n) and n-1 hydroxy-PUFA or to epoxy-PUFA [6]. Epoxy-PUFA are further metabolized to dihydroxy-PUFA by soluble epoxide hydrolase (sEH) [7]. Hydro(pero)xy-PUFA and prostaglandin-like structures, called isoprostanes (IsoP), are also formed during autoxidative processes [8,9]. The biology of free oxylipins has been investigated in numerous studies over the past decades [1–3]. For instance, PGE_2, a prostaglandin formed from arachidonic acid (ARA, C20:4 n6) via COX, is a potent mediator in the regulation of pain, fever and inflammation [4], e.g. by arterial dilation and increase of microvascular permeability leading to increased blood flow in the inflammation site or by interaction with EP1 receptor having an effect on neurons at the inflammation site resulting in hyperalgesia [10,11]. In contrast, epoxy-

* Corresponding author. Chair of Food Chemistry, Faculty of Mathematics and Natural Sciences, University of Wuppertal, Gaußstr. 20, 42119, Wuppertal, Germany.
E-mail address: nils@schebb-web.de (N.H. Schebb).
[1] Authors contributed equally.

https://doi.org/10.1016/j.talanta.2020.121074
Received 19 November 2019; Received in revised form 20 April 2020; Accepted 21 April 2020
Available online 25 April 2020
0039-9140/

Abbreviations

AdA	adrenic acid
ALA	α-linolenic acid
ARA	arachidonic acid
BHT	butylated hydroxytoluene
CI	confidential interval
COX	cyclooxygenase
CV	coefficient of variation
CYP	cytochrome P450 monooxygenase
DGLA	dihomo-γ-linolenic acid
DHA	docosahexaenoic acid
DiHDPE	dihydroxy-docosapentaenoic acid
DiHETE	dihydroxy-eicosatetraenoic acid
DiHETrE	dihydroxy-eicosatrienoic acid
DiHOME	dihydroxy-octadecenoic acid
EA	ethyl acetate
EDTA	ethylenediamine-tetraacetic acid
EPA	eicosapentaenoic acid
EpDPE	epoxy-docosapentaenoic acid
EpETE	epoxy-eicosatetraenoic acid
EpETrE	epoxy-eicosatrienoic acid
EpOME	epoxy-octadecenoic acid
GLA	γ-linolenic acid
HDHA	hydroxy-docosahexaenoic acid
HEPE	hydroxy-eicosapentaenoic acid
HETE	hydroxy-eicosatetraenoic acid
HOAc	acetic acid
HODE	hydroxy-octadecadienoic acid
HOTrE	hydroxy-octadecatrienoic acid
IS	internal standard
isoP	isoprostane
LA	linoleic acid
LLOQ	lower limit of quantification
LOD	limit of detection
LOX	lipoxygenase
LT	leukotriene
Lx	lipoxine
MeOH	methanol
n3-DPA	n3-docosapentaenoic acid
NSAIDs	non-steroidal anti-inflammatory drugs
OA	oleic acid
oxo-ETE	oxo-eicosatetraenoic acid
oxo-ODE	oxo-octadecadienoic acid
oxo-OTrE	oxo-octadecatrienoic acid
PG	prostaglandin
PUFA	polyunsaturated fatty acid
QS	quality standard
RBC	red blood cells
Rv	resolvin
sEH	soluble epoxide hydrolase
SPE	solid phase extraction
SPM	specialized pro-resolving lipid mediator
t-AUCB	*trans*-4-(-4-(3-adamantan-1-yl-ureido)-cyclohexyloxy)-benzoic acid
TriHODE	trihydroxy-octadecadienoic acid
TriHOME	trihydroxy-octadecenoic acid
Tx	thromboxane
ULOQ	upper limit of quantification

PUFA formed via CYP from ARA, eicosapentaenoic acid (EPA, C20:5 n3) and docosahexaenoic acid (DHA, C22:6 n3) have anti-inflammatory properties [12]. Epoxy-PUFA are also involved in several biological processes like vasodilation, angiogenesis and hypertension [13]. However, epoxy-PUFA are rapidly metabolized by sEH to their corresponding dihydroxy-PUFA which are less active [13,14].

Several studies investigated the modulation of oxylipin synthesis via nutrition or therapeutic treatment. Nutritional intervention by supplementation of n3-PUFA on a Western diet leads to a shift in the relative proportions of n3- and n6-PUFA influencing the oxylipin profile due to variable affinity of the PUFA metabolizing enzymes to the various PUFA and changes in the substrate availability [15–19]. The expression and/or activity of enzymes involved in the ARA cascade can further be modified by drug intervention leading to altered oxylipin profiles [1]. For instance, COX can be inhibited competitively by non-steroidal anti-inflammatory drugs (NSAIDs) or in case of the NSAID aspirin irreversibly through acetylation of serine at the active enzyme site [11,20]. Moreover, food derived secondary products like polyphenols can affect the enzyme activity resulting in altered oxylipin patterns [1]. For example, the activity of CYP can be altered *in vitro* by the polyphenol apigenin [21] and the activity and the expression of COX-2 can be influenced by resveratrol, hopeaphenol and apigenin [22].

The influence of these potent lipid mediators on health and disease as well as the interaction with nutrition or drugs have been investigated in numerous clinical studies. However, the results can be massively affected by (unsuitable) sample handling, e.g. artificial formation of oxylipins during sample preparation, ion suppression due to insufficient removal of interfering matrix [1,23–25] or inefficient extraction of oxylipins from biological samples [1].

Besides analytical challenges, the stability of oxylipins is crucial because samples are often stored for different periods of time prior to analysis in daily clinical routine or longitudinal studies. However, only few reports exist on the influence of the transitory stage between blood collection and plasma generation on the oxylipin profile. First studies revealed that the apparent pattern of free oxylipins changes depending on storage procedures of whole blood [22,26] or plasma [27]. However, the reported results are conflicting, e.g. Dorow et al. found all detectable oxylipins being stable in EDTA-whole blood up to 120 min at 4 °C [26], while Willenberg et al. showed reduced concentrations of hydroxy-PUFA at storage times longer than 60 min at 4 °C [22].

Similarly, little is known about the impact of storage conditions on the profile of total oxylipins. However, the data are urgently needed since the major part of epoxy- and hydroxy-PUFA as well as isoprostanes are found to be esterified in lipids [28,29]. Total oxylipins might be a good option in the field of biomarker discovery as they represent the plasma oxylipin pattern, might be biologically active and their levels fluctuate depending on lipoprotein concentration and composition [1].

In the present study we employed a comprehensive liquid chromatography-tandem mass spectrometry (LC-MS/MS) method covering 133 analytes to evaluate the sample preparation/storage induced effects on the pattern of plasma oxylipins. We investigated the efficacy of different additives to prevent artificial formation of oxylipins during sample preparation. Additionally, we monitored the impact of different storage times and temperatures at different stages of plasma generation, which are representative for current practices in clinics, on the apparent total plasma oxylipin concentrations. Finally, we examined the long-term stability of total oxylipins in plasma stored at −80 °C during a period of 15 months.

2. Materials and methods

2.1. Chemicals

The analyte standards 10-HODE, 12-HODE, 15-HODE, 13-oxoOTrE, 9,10,11-TriHOME, 9,12,13-TriHOME, 9,10,13-TriHOME, 9,10,11-

TriHODE, 9,12,13-TriHODE and 9,10,13-TriHODE were purchased from Larodan (Solna, Sweden). All other oxylipin standards and deuterated internal standards were bought from Cayman Chemical (local distributor Biomol, Hamburg, Germany). LC-MS grade acetic acid, acetonitrile, *iso*-propanol and methanol (MeOH) were obtained from Fisher Scientific (Schwerte, Germany). HPLC grade *n*-hexane was purchased from Carl Roth (Karlsruhe, Germany) and HPLC grade ethyl acetate was purchased from VWR (Darmstadt, Germany). The ultrapure water (> 18 MΩ*cm) was generated by the Barnstead Genpure Pro system from Thermo Fisher Scientific (Langenselbold, Germany).

2.2. Generation of the quality standard (QS) plasma

Human EDTA-blood was collected from 4 to 6 healthy male and female individuals aged between 25 and 38 years. The blood was centrifuged (1200 × *g*, 15 min, 4 °C), the collected plasma supernatants were pooled, aliquoted and immediately stored at −80 °C as quality standard (QS) plasma.

2.3. Calibration

A wide range of oxylipins from different structural classes and derived from different precursor fatty acids (ARA, EPA, DHA, dihomo-γ-linolenic acid (DGLA, C20:3 n6), adrenic acid (AdA, C22:4 n6), n3- and n6-docosapentaenoic acid (DPA, C22:5 n3/n6), γ-linolenic acid (GLA, C18:3 n6), α-linolenic acid (ALA, C18:3 n3), linoleic acid (LA, C18:2 n6) and oleic acid (OA, C18:1 n9)) were selected for calibration. Only alkali stable prostanoids, such as B-ring or F-ring prostaglandins, were included in the calibration. For the quantification of oxylipins the deuterated internal standards $^{2}H_4$-6-keto-$PGF_{1\alpha}$, $^{2}H_4$-8-*iso*-$PGF_{2\alpha}$, $^{2}H_4$-$PGF_{2\alpha}$, $^{2}H_5$-RvD2, $^{2}H_{11}$-8,12-*iso*-$iPF_{2\alpha}$-VI, $^{2}H_5$-LxA_4, $^{2}H_5$-RvD1, $^{2}H_4$-PGB_2, $^{2}H_4$-LTB_4, $^{2}H_4$-9,10-DiHOME, $^{2}H_{11}$-11,12-DiHETrE, $^{2}H_6$-20-HETE, $^{2}H_4$-13-HODE, $^{2}H_4$-9-HODE, $^{2}H_8$-15-HETE, $^{2}H_3$-13-oxo-ODE, $^{2}H_8$-12-HETE, $^{2}H_8$-5-HETE, $^{2}H_4$-12(13)-EpOME, $^{2}H_{11}$-14(15)-EpETrE, $^{2}H_7$-5-oxo-ETE, $^{2}H_{11}$-8(9)-EpETrE were used. Before pipetting of the calibration standards, purity and concentration of all analyte standards were controlled according to Hartung et al. [30]. The preparation of the calibration series is described in detail in the Supporting Information (Tables S1 and S2, Fig. S1). Validation criteria of the European Medicines Agency (EMA) guidelines for bioanalyses were considered during method development [31].

2.4. Preparation of samples for storage assays

Short-term transitory storage assay: Blood from 4 healthy volunteers aged 25–30 years was collected in EDTA-monovettes (S-Monovette K3E, 02.1066.001, Sarstedt, Nümbrecht, Germany). The subjects did not take NSAIDs. Blood from each individual was pooled, aliquoted and submitted to different treatments before final storage at −80 °C (Table 1). “Best case” samples were immediately centrifuged (10 min, 4 °C, 1200 × *g*), the plasma was collected, snap-frozen in liquid nitrogen and stored at −80 °C until further analysis. “Vortex” samples were strongly shaken (Vortex Genie 2, Scientific Industries (local distributor Carl Roth, Karlsruhe, Germany) max. intensity) for 1 min directly after blood withdrawal, centrifuged (10 min, 4 °C, 1200 × *g*), the plasma was frozen in liquid nitrogen and stored at −80 °C until further analysis. The influence of storage conditions was investigated in three different ways:

1. Whole blood was stored at room temperature (20 °C) or in the fridge (4 °C) for different time periods, centrifuged plasma was collected and stored at −80 °C until analysis.
2. Whole blood was directly centrifuged, stored at 4 °C for different periods of time, plasma was collected and stored at −80 °C until analysis.
3. Whole blood was directly centrifuged, plasma was collected and temporarily stored at 4 °C or at −20 °C for different time periods and finally stored at −80 °C until analysis.

Additionally, a “worst case” sample was prepared that combines the longest time periods of all three storage conditions described above. Samples from each individual were prepared and analyzed separately together with two QS plasma samples as a quality control.

Long-term storage assay: The human EDTA-plasma used for long-term storage experiments was bought from Etablissement Français du Sang (Saint-Denis, France; pool of 50 donors) aliquoted and stored at −80 °C untill analysis. The samples were prepared in triplicates together with 3 QS plasma samples as a quality control. In the first 6 months of the long-term storage experiment plasma samples were prepared and analyzed every month and thereafter every three months (month 9, 12 and 15).

2.5. Sample preparation and LC-ESI(-)-MS/MS analysis

Human plasma samples were extracted using solid phase extraction (SPE) following protein precipitation and alkaline hydrolysis as described [32] and in detail in the SI. Samples were analyzed by means of LC-ESI(-)-MS/MS (Table S3) as described [33,34].

In order to investigate the effects of the compounds included in the antioxidant mixture each compound (butylated hydroxytoluene, BHT

Table 1
Overview of the sampling design to investigate the influence of storage at transitory stages on the oxylipin pattern. Blood from 4 individuals was collected into EDTA tubes, aliquoted and submitted to different subsequent treatments before final storage at – 80 °C. Best case samples were immediately centrifuged and frozen. Other samples were stored at room temperature or at 4 °C for different time periods before centrifugation. After centrifugation samples were stored at 4 °C without removing the plasma supernatant and at 4 °C as well as room temperature after plasma separation. Additionally, one sample from each individual was vigorously shaked “vortex” for 1 min to provoke hemolysis.

	Sample collection	Vortexing	Storage before centrifugation		centrifugation	Storage after centrifugation			Storage at −80°C
			20°C (RT)	4°C (fridge)		Plasma NOT separated	Plasma separated		
						4°C	4°C	-20°C	
Best case (directly -80°C)		-	-	-		-	-	-	
Storage before centrifugation		-	1 h, 2 h, 3 h	-		-	-	-	
		-	-	1 h, 8 h, 24 h		-	-	-	
Storage after centrifugation		-	-	-		1 h, 2 h	-	-	
		-	-	-		-	1 h, 2 h, 8 h, 24 h	-	
		-	-	-		-	-	8 h, 24 h, 3 d, 5 d	
		-	-	-		-	1 h	3 d	
Shaking of sample		1 min	-	-		-	-	-	
Worst case		-	3 h	24 h		2 h	2 h	5 d	

and EDTA, each 0.2 mg/mL and indomethacin and *trans*-4-(-4-(3-adamantan-1-yl-ureido)-cyclohexyloxy)-benzoic acid, *t*-AUCB, each 100 μM) was added individually and in combination to QS plasma samples.

2.6. Data analysis

Inter-individual analyte variance in oxylipin patterns [1,19] was compensated by normalizing the oxylipin level against the respective oxylipin concentration in the "best case" samples (i.e. directly processed samples) determined in triplicate for each subject. The results are shown as mean (%) ± 95% confidence interval (CI). Normal distribution was shown using the Shapiro-Wilk test. Outliers were identified using the ROUT (Robust regression and OUTlier removal, maximum false discovery rate (Q) = 1%) outlier test and removed. The variability of all conditions was assessed by an unsupervised multivariate analysis, a principal component analysis (PCA). The differences between best case and storage conditions were determined by one-way ANOVA following Tukey post-test. p values < 0.05 were considered significant.

Long-term storage data were evaluated firstly by controlling if the concentrations were comprised within a range of acceptable analytical variance of ± 30% relative to month 1 of the monitoring. Then data were evaluated using linear regression model for each oxylipin. The hypothesis of residuals independence, normality and homogeneity was tested to validate the linear models (using Durbin-Watson test, Shapiro-Wilk test and non-constant error variance test, respectively). The significance of the slope of each linear regression model was calculated with a *t*-test, p-values < 0.05 were considered significant. For the oxylipins, which show a significant slope, the trend line was inserted into the respective diagram.

Statistical analyses were performed using GraphPad Prism software (version 6.0, San Diego, CA; USA), R software or SIMCA (version 14, Umetrics). All other calculations were done with Excel Microsoft Office (version 365, Redmond, WA, USA).

3. Results

3.1. Effects of additives on the oxylipin pattern

The addition of BHT before sample preparation yielded significantly lower apparent concentrations of hydroxy-PUFA (Fig. 1A; Table S4) whereas levels of epoxy-PUFA were mostly unaffected (Fig. 1B, Table S4). For EDTA no effects on the plasma oxylipin pattern were observed (Fig. 1). Similarly, the enzyme inhibitors indomethacin (COX-1/-2) and *t*-AUCB (sEH) did not change the apparent oxylipin pattern (Fig. 1). The results obtained following addition of an antioxidant mixture containing all four tested additives (BHT, EDTA, indomethacin and t-AUCB) were consistent with the results yielded with BHT addition alone.

3.2. Oxylipin concentrations in plasma

Quality standard (QS) plasma was prepared and analyzed with each data set. The concentrations of total oxylipins in QS plasma are presented in the Table S5. In this pooled human plasma 78 analytes could be quantified in the range of 150 ± 40 pM (11,12-DiHETE and 14,15-DiHETE) to 186 ± 53 nM (9(10)-Ep-stearic acid). The LLOQ in plasma ranged from 5 pM (9,10-DiHOME) to 500 pM ($PGF_{3\alpha}$ or 8,15-DiHETE) for most of the analytes. Only for 15-F_{3t}-IsoP, 13-γ-HOTrE, 19-HETE, 17-oxo-DPA (n3) and 17-oxo-DHA the method was less sensitive (LLOQ 1.25–5 nM). Regarding intra-day and inter-day variance, for most of the quantified analytes the coefficient of variation (CV) was < 20% and thus slightly higher than for the determination of free oxylipins [35]. For epoxy-PUFA high variations of > 30% were observed.

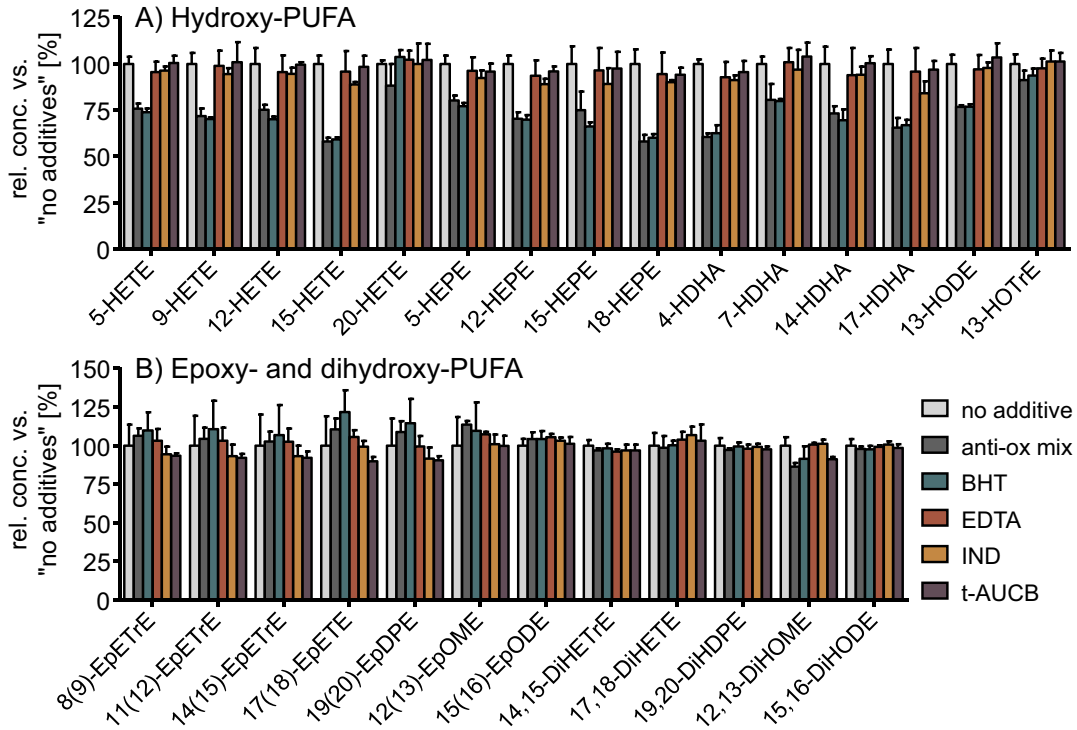

Fig. 1. Effects of additives on the apparent oxylipin pattern. Shown are relative oxylipin concentrations of a representative set of analytes using different additives during sample preparation (mean ± SD; n = 4). Samples were prepared using no additives, butylated hydroxytoluol (BHT), ethylenediamine-tetraacetic acid (EDTA), indomethacin (IND) and the sEH inhibitor *t*-AUCB, respectively or a mix containing all additives (anti-ox mix). Relative concentrations were calculated against the mean analyte concentration obtained from sample preparation without additives (no additives). Statistical differences between "no additive" and different additives were evaluated by two-way ANOVA followed by Bonferroni post-test (Table S4).

3.3. Transitory stage of plasma generation

In the best case plasma samples 78 oxylipins could be quantified with concentrations ranging from 149 ± 54 pM (14,15-DiHETE) to 158 ± 65 nM (9(10)-Ep-stearic acid, Table S6). The concentrations of all detected oxylipins at all time points can be found in the SI (Table S6). The PCA, unsupervised multivariate analysis, shows the variability of the all dataset (R^2X = 0.799 and Q^2 = 0.506, Fig. S2). As shown in the score plot (Fig. S2 A), the condition "worst case" is the main contributor of the variability of the dataset (i.e. concentrations of the 78 oxylipins) on the first component that brings 48% of the variability. On the second component bringing 19% of the variability, the effect of "vortex" seems to be also significant. The loading plot (Fig. S2 B) reveals that the condition "worst case" mostly increase the concentration of hydroxy-PUFAs (e.g. 5-HETE, 20-HDHA, …) whereas the "vortex" affects particularly all epoxy-PUFAs of the dataset. Among all these oxylipins, several oxylipins were selected which represent the four branches of the arachidonic acid cascade [1,2] and can therefore be used to study the effect of different storage conditions on the oxylipin profile. The influence of transitory stage after blood collection until storage of plasma at −80 °C on the oxylipin pattern in plasma is shown exemplarily as fold change relative to immediate processing for a representative set of oxylipins (Fig. 2). The concentration of most of the representative analytes did not change markedly at the various storage conditions. The levels of the products derived from LOX catalyzed reactions (such as 5-, 12- and 15-HETE) and of the presumably autoxidatively formed products (such as 9-HETE and 5(*R*,*S*)-F_{2t}-IsoP) were slightly (1.2–1.5 fold) increased when plasma was stored at 4 °C after centrifugation and > 1.5 fold elevated for the worst case scenario (Fig. 2). The epoxy-PUFA concentrations were generally increased at prolonged storage times at elevated temperatures in comparison to the best case scenario. These trends were also reflected by the mean ± 95% CI of the concentrations for representative oxylipins derived from ARA, EPA, DHA, LA and ALA calculated against concentration in the best case sample (relative concentrations, Fig. 3, Figs. S3–8). 5-HETE, 12-HETE and 15-HETE reached the highest levels in the worst case sample (1.8–3.5-fold increase) which were also significantly different from the best case sample (Fig. 3A–C). This accumulative effect towards worst case and the significant difference of the concentrations compared to best case could also be observed for 5-, 12- and 15-LOX products derived from other PUFA (Figs. S3–6, Table S6). For 14(15)-EpETrE no significant changes in the concentrations could be detected at any storage condition, however the variance was massively increased, e.g. when plasma was stored for 1 h or 6 h at 4 °C (Fig. S9). These strong variations of the concentrations of 14(15)-EpETrE during different storage conditions (Fig. 3F) were also detected for other epoxy-PUFA (Fig. S7). Levels of the isoprostane 5(*R*,*S*)-5-F_{2t}-IsoP varied in a similar range (Figs. 2 and 3D, Fig. S8) while dihydroxy-PUFA such as 14,15-DiHETrE were not influenced by the storage (Figs. 2 and 3E, Fig. S7).

3.4. Long-term storage of plasma

In plasma samples used to evaluate the effect of long-term storage (at −80 °C, up to 15 months) on the stability of different oxylipin types 74 oxylipins could be quantified (Table 2, Fig. S10). Considering that an analytical variance of 20% up to ± 30% is acceptable, 69 oxylipins (93% of the quantified oxylipins) were considered to be stable during the 15 months of monitoring (Table S7). Nevertheless, the concentration of some oxylipins changed over time. On the one side, the concentration of 17 oxylipins (hydroxy-PUFAs) significantly increased (Table 2, left hand side, highlighted in grey) among which 13-HODE and 9-HETE had the highest coefficients of slope. When considering the difference between month 15 and month 1, the difference of plasma concentration was more pronounced for 9-HETE (+25%) than for 13-HODE (+7%). Importantly, 9-HETE and 8,15-DiHETE were the only two oxylipins for which the change of the concentrations over the investigated period exceeded the threshold of analytical variance (± 30%, Fig. 4). Of note, the concentration of the isoprostane 5(*R*,*S*)-F_{2t}-IsoP remained stable over time (non-significant coefficient of slope and concentrations within the range of ± 30%). On the other side, the concentration of 8 oxylipins significantly decreased during the 15 months of monitoring (Table 2, right hand side, highlighted in grey). These oxylipins are all derived from the CYP pathway and 15(16)-

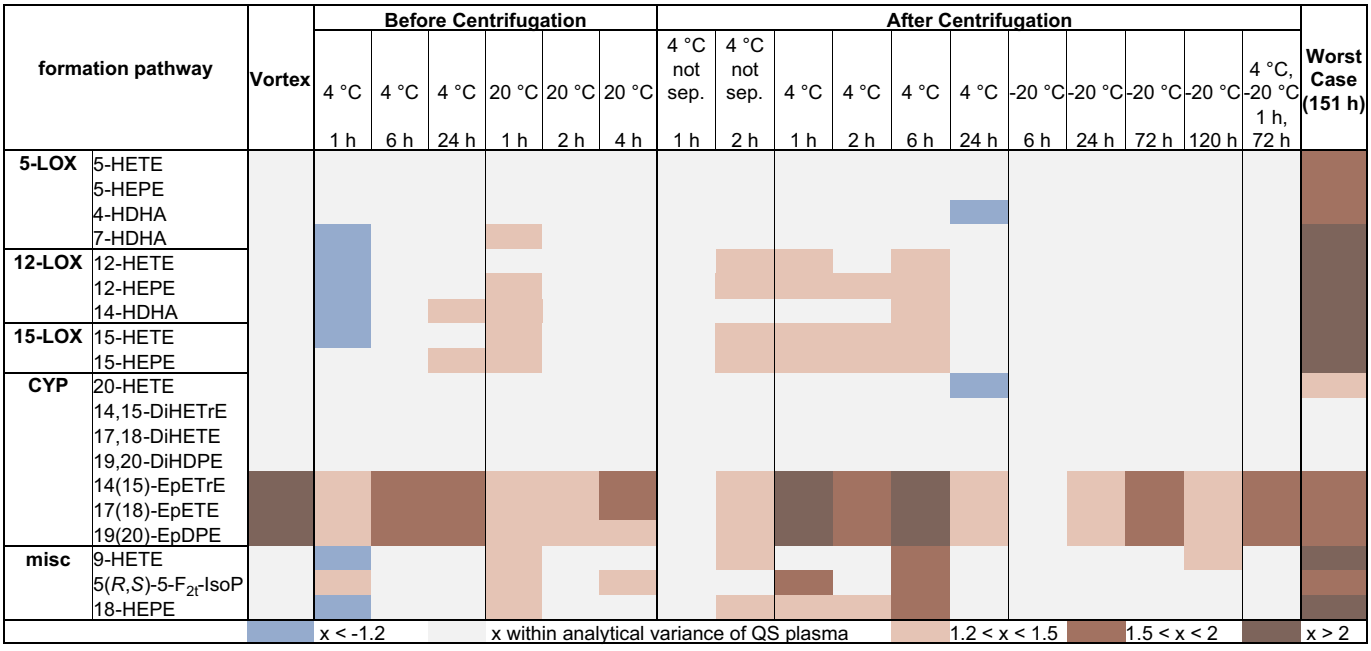

Fig. 2. Effects of different storage conditions on the total oxylipin concentration. The heatmap shows the fold change of the mean concentration for representative analytes relative to mean concentration of best case (processed immediately). Marked in grey are samples within the analytical variance (± 20%) of QS plasma. Blue represents a decrease of > 1.2-fold against the "best case". An increase is highlighted in the different shades of red (light red 1.2–1.5-fold; red 1.5–2.0-fold; dark red > 2-fold). (For interpretation of the references to colour in this figure legend, the reader is referred to the Web version of this article.)

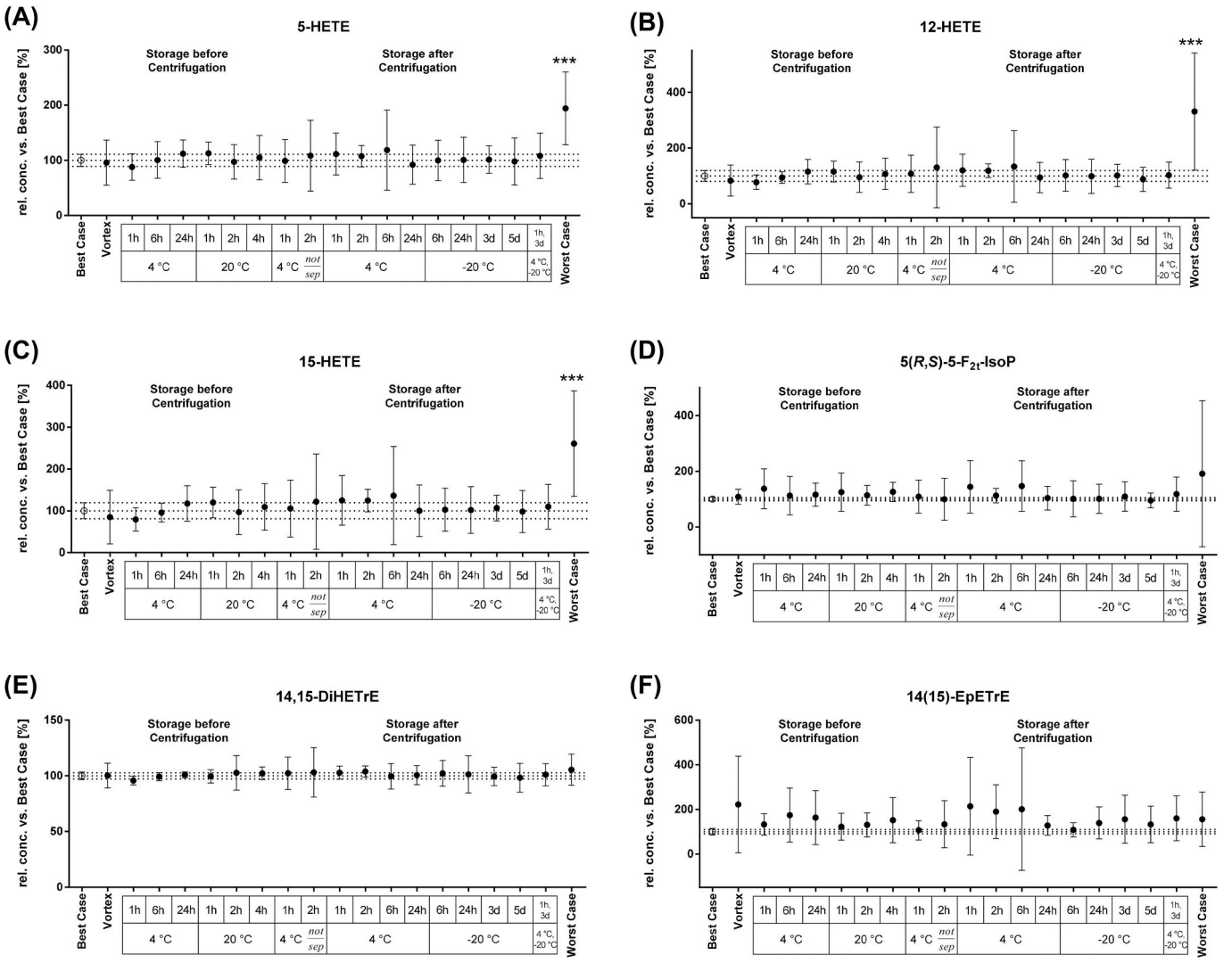

Fig. 3. Stability of total oxylipins during plasma generation with different transitory storage times. The relative concentrations of selected ARA derived oxylipins (A) 5-HETE, (B) 12-HETE, (C) 15-HETE, (D) 5(*R*,*S*)-5-F_{2t}-IsoP, (E) 14,15-DiHETrE and (F) 14(15)-EpETrE were calculated against the concentration of the best case. Shown are mean ± 95% CI (n = 4–12). The dotted lines mark the 95% CI of the best case scenario. Statistical differences between best case and different storage conditions were evaluated by one-way ANOVA followed by Tukey post-test (***p < 0.001). The data for oxylipins derived from other precursor PUFA (ARA, EPA, DHA, ALA, LA) can be found in the SI.

EpODE as well as 12,13-DiHOME had the lowest coefficients of slope. When considering the difference between month 15 and month 1, the plasma concentrations of 15(16)-EpODE and 12,13-DiHOME decreased by 21% and by 14%, respectively. Finally, 8(9)-EpETE was the only oxylipin which exceeded the threshold of analytical variance (± 30%, Fig. 4).

4. Discussion

Oxylipins are formed from polyunsaturated fatty acids which can easily be oxidized. Therefore, in the analysis of oxylipins in biological samples such as blood particular attention should be paid to their stability during plasma generation, storage and sample handling. Only a few studies have been published investigating the influence of the plasma generation procedure and long-term storage on the profile of oxylipins [22,26,27]. However, these studies only evaluated free, i.e. non-esterified oxylipins. A major part of oxylipins occurs esterified in biological samples, e.g. bound in lipids [28,36] and a large number of studies utilizes the total oxylipin pattern to understand the biology of the oxylipins [1,18,22].

Our study is the first one investigating the stability of total oxylipins with respect to sample collection, preparation and storage. We assessed the effect of different additives prior to sample preparation, the effect of different duration and temperature during plasma generation as well as the effect of long-term storage on a large pattern of oxylipins using one of the most comprehensive targeted metabolomic platforms (quantitative analysis of > 133 oxylipins) available.

Influence of additive addition prior to sample preparation. Additives are commonly added before analytical sample preparation to avoid degradation and artifact formation [22,33,37]. Indeed, the addition of BHT at the beginning of sample preparation resulted in a reduction of apparent hydroxy-PUFA concentrations in comparison to samples prepared without additives. The antioxidant BHT reduces peroxyl radical oxidation of PUFA [38] and is therefore commonly used to quench radical catalyzed reactions [39] resulting in a reduction of autoxidative processes. The autoxidation of PUFA is initiated by free radical hydrogen abstraction at a bis-allylic position resulting in a hydroperoxy-PUFA that is reduced to the corresponding hydroxy-PUFA. In case of ARA 8-, 9-, 11-, 12- and 15-H(p)ETE can be formed [40] whereas for EPA hydrogen is primarily abstracted at positions C7, C10, C13 or C16

Table 2
Slopes coefficients (left: positive slope, right: negative slope) and associated p-value from the linear regression models for each oxylipin. Oxylipins with a significant evolution (p-val < 0.05) during the long-term storage are highlighted in grey and sorted by the coefficient of slope.

Oxylipins	Coefficient of positive slope	p-value	Oxylipins	Coefficient of negative slope	p-value
13-HODE	2.0440	0.0055	15(16)-EpODE	-0.8775	0.0345
9-HETE	0.9167	0.0107	12,13-DiHOME	-0.3957	0.0068
12-HETE	0.6325	0.0136	8(9)-EpETE	-0.0458	0.0124
11-HETE	0.5885	3.00E-04	20-HETE	-0.0440	0.0151
8-HETE	0.4874	3.00E-04	20-HEPE	-0.0359	0.0247
8-HDHA	0.4538	0.0123	19,20-DiHDPE	-0.0236	0.0058
17-HDHA	0.4276	0.0012	14(15)-DiHETrE	-0.0087	0.0025
15-HETE	0.3777	0.0175	11(12)-DiHETE	-0.0021	0.0108
15(S)-HETrE	0.2190	0.0304	12(13)-EpOME	-1.1686	0.0548
14-HDHA	0.2183	0.0248	5(6)-EpETrE	-0.5579	0.4088
9-HEPE	0.2018	0.0028	9(10)-EpOME	-0.3766	0.3078
20-HDHA	0.1491	0.0275	9,10-DiH-stearic acid	-0.3451	0.2094
13-HDHA	0.1455	0.0011	5(6)-DiHETrE	-0.1522	0.1221
11-HDHA	0.1325	0.0091	14(15)-EpETrE	-0.1388	0.4754
16-HDHA	0.1096	0.0132	7-HDHA	-0.0959	0.0694
8,15-DiHETE	0.0461	0.0097	11(12)-EpETrE	-0.0953	0.4629
10-HDHA	0.0450	0.0309	9-HOTrE	-0.0688	0.2634
9(10)-Ep-stearic acid	3.6023	0.1841	19(20)-EpDPE	-0.0617	0.1646
9-HODE	0.4128	0.6896	9,10-DiHOME	-0.0605	0.1888
5-HETE	0.3128	0.0835	8(9)-DiHETrE	-0.0382	0.2585
21-HDHA	0.0624	0.2058	19-HEPE	-0.0370	0.0864
4-HDHA	0.0606	0.4082	12-HHTrE	-0.0369	0.4040
13-HOTrE	0.0539	0.1937	15-HEPE	-0.0338	0.1176
18-HEPE	0.0530	0.1619	9(10)-EpODE	-0.0305	0.0781
12-HEPE	0.0504	0.3281	12(13)-EpODE	-0.0280	0.1811
11-HEPE	0.0462	0.4821	10(11)-EpDPE	-0.0268	0.5585
15,16-DiHODE	0.0362	0.8049	8(9)-EpETrE	-0.0220	0.7249
8-HEPE	0.0282	0.2762	14(15)-EpETE	-0.0150	0.4343
5-HEPE	0.0213	0.3121	7,8-DiHDPE	-0.0137	0.5564
5(S)-HETrE	0.0169	0.0962	17(18)-EpETE	-0.0112	0.4341
16(17)-EpDPE	0.0135	0.5110	11(12)-DiHETrE	-0.0092	0.1581
4,5-DiHDPE	0.0117	0.7976	10,11-DiHDPE	-0.0066	0.1818
9,10-DiHODE	0.0040	0.4161	8(9)-DiHETE	-0.0057	0.1479
17(18)-DiHETE	0.0012	0.7127	16,17-DiHDPE	-0.0049	0.1034
13(14)-EpDPE	0.0003	0.9924	13,14-DiHDPE	-0.0038	0.2535
14(15)-DiHETE	0.0002	0.7934	5(R,S)-F2t-IsoP	-0.0030	0.5571
			22-HDHA	-0.0007	0.9718
			12,13-DiHODE	-0.0002	0.9839

[25,41]. Consistently, after addition of BHT we observed a reduction of almost all hydroxy-PUFA with a slight preference for 15-HETE and 18-HEPE whereas 20-HETE was not affected (Fig. 1).

Neither EDTA nor indomethacin nor *t*-AUCB influenced the apparent oxylipin concentrations. It is likely that protein precipitation with *iso*-propanol which is the first step during sample preparation is sufficient to remove residual enzyme activity in plasma, however inhibition of enzymes involved in oxylipin formation might be relevant for other samples like tissues or other sample preparation strategies. Indomethacin is a non-selective COX-1 and COX-2 inhibitor [42] and is added in order to suppress *ex vivo* formation of prostanoids. Since the majority of COX products is base labile, the effect of indomethacin was hard to deduce in our data set, and inhibition of COX seems to be less relevant for determination of total oxylipins in plasma. However, free oxylipin levels might be influenced by residual COX activity. The metabolism of epoxy-PUFA to vicinal dihydroxy-PUFA by sEH can be prevented by the use of inhibitors such as *t*-AUCB [43]. Particularly, in samples with high sEH activity such as liver or kidney tissue [44] the addition of an inhibitor before homogenization and lipid extraction can be relevant. EDTA can serve as a chelator of metal ions in particular of iron ions which promote lipid peroxidation [45] and of calcium ions which activate phospholipase A_2 [46]. However, it is poorly soluble in MeOH and thus may not be included in the additive mixture. Overall, our results show that the different aspects of the sample preparation procedure may have a relevant impact on the apparent oxylipin concentrations. Particularly, the addition of antioxidants like BHT is crucial in order to minimize the artificial formation of oxylipins during sample preparation.

Stability of oxylipins during the transitory stage of plasma generation. Human whole blood contains in addition to the plasma/serum several blood cell types namely erythrocytes, leukocytes and platelets. Most of the enzymes of the ARA cascade are expressed in blood and immune cells. For instance, 5-LOX is expressed in activated polymorphonuclear leukocytes (PMNL) or monocytes [47,48]. In platelets active 12-LOX and COX-1 can be found [49,50] whereas 15-LOX can be expressed in macrophages [51]. Additionally, COX-2 is expressed in activated monocytes [52].

Particularly, platelets and thus 12-LOX metabolites are often considered to cause alteration in the apparent plasma oxylipin pattern through unsuitable plasma preparation and storage. Therefore, the required steps during the generation of plasma should be performed immediately in order to minimize *ex vivo* metabolism. In large study cohorts or daily clinical routine, direct processing of collected whole blood is often not possible resulting in longer periods of time during the transitory stage. Here, we demonstrate that the concentrations of all oxylipin classes remained almost stable during the transitory stage and

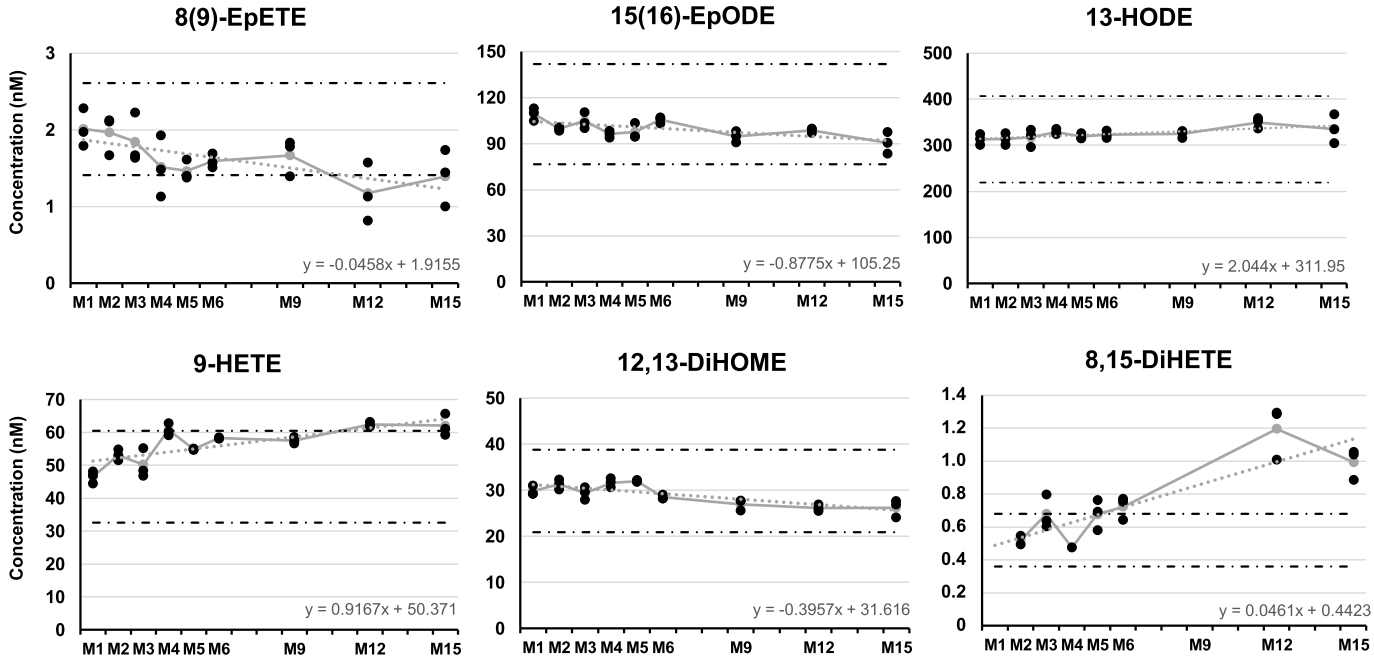

Fig. 4. Long-term storage evaluation over 15 months for oxylipins with significant slopes (positive and negative, n = 25). The black dotted lines mark the ± 30% of acceptable analytical variance. Black dots represent the samples. Grey dots are the mean of samples by month and a grey line connects these means. The grey dotted lines are the straight linear regression with the mathematical equation shown near the name of oxylipins.

only drastic intervention in the storage conditions (as it was performed in the worst case) resulted in significantly increased oxylipin levels particularly of hydroxy-PUFA (Fig. 3, Figs. S3–8). The worst case included delays in all steps of plasma generation with a total duration of 151 h before freezing at -80 °C. It should be noted that apart from the worst case scenario the highest effect of this transitory storage was an increase of epoxy-PUFA by factor 2. Even though a combination of different storage conditions affected the total oxylipin concentration, no clear correlation between storage time, temperature or stage of plasma generation and the total oxylipin concentration was observable. Nevertheless, some trends can be deduced. The concentrations of the 5-/12-/15-LOX metabolites derived from ARA, EPA and DHA were reduced when whole blood was stored at 4 °C for 1 h compared to baseline and increased during 24 h. Additionally, the increased concentrations of products derived from 12- and 15-LOX when storing whole blood for 24 h at 4 °C may be caused by platelet activation. Although the blood cells are separated from the plasma by centrifugation, residual LOX activity or autoxidation might also lead to increased concentrations of 12- and 15-LOX metabolites when samples were stored at 4 °C after centrifugation before as well as after plasma separation. However, one would assume that this happens more in whole blood than in plasma. It can be assumed that (intact) platelets are efficiently removed by centrifugation at 1200 × *g* for 10 min [53], too harsh centrifugation might also lead to platelet activation [54]. Furthermore, plasma generated from chilled whole blood, as it was performed in our study, has been reported to contain lower concentrations of platelet derived oxylipins due to possibly slowed enzymatic activity and/or cold-induced aggregation of platelets *ex vivo* leading to more efficient removal [55,56].

Additionally, unsuitable blood handling may cause hemolysis, i.e. the release of hemoglobin upon disruption or damage of erythrocyte membranes [57] which might lead to increased oxylipin concentrations e.g. by Fenton-type catalyzed autoxidation [55]. In case of the vortexed samples which was intended to simulate hemolysis no increase in the concentrations was observed. However, this may also indicate that the sample treatment was not sufficient to cause hemolysis.

The effects of storage temperature and time with regard to the pattern of free oxylipins have been previously described [22,26,27,58]. These studies revealed a clear effect of sample storage at temperatures above −80 °C on the free oxylipin pattern. In a study by Jonasdottir et al. most of the free oxylipins were stable up to 120 min at 4 °C in whole blood and plasma whereas 9-HETE increased after 60 min at 4 °C. Also, the storage of whole blood at room temperature led to higher concentrations of 12-HETE and 12-HHTrE after storing for 30 min [26]. Ramsden et al. also described the increase of 12-LOX and platelet derived oxylipins in whole blood at room temperature in a time dependent manner, whereas storage on ice for up to 2 h had no effect on oxylipin concentrations [58]. However, in Willenberg et al. the concentrations of 11-HETE, 15-HETE, $PGF_{2\alpha}$, 11(12)-EpETrE and 14(15)-EpETrE were reduced by half in plasma and whole blood after 60 min when stored at room temperature or on ice whereas other oxylipins remained stable [22]. In contrast, Jonasdottir et al. reported that several hydroxy-PUFA were significantly increased in plasma after 8 h at room temperature, while no significant differences could be observed at 6 °C up to 24 h. 12-HETE was massively increased after 24 h at −20 °C [27]. Of note, these studies differ regarding their used analytical method which influences the apparent oxylipin concentrations [22,59].

Although our results for total oxylipins indicate that oxylipins can be considered to be stable during the transitory stage, it cannot be ruled out that oxylipin levels might be affected in other studies. Especially the blood of non-healthy participants might have higher concentrations of released precursor PUFA or ARA cascade enzymes [1]. Thus, this blood samples might be more prone to storage induced changes. The only way to reduce the potential risk of an artificially changed oxylipin pattern is to perform all steps between blood withdrawal and freezing of the plasma samples as soon as possible and as comparable as possible between the study samples. This also contributes to lower variances of oxylipin concentrations close to the analytical variance. Though there was no significant increase in the concentrations during storage higher coefficients of variations were observed for some storage conditions. Storage of centrifuged plasma for 2 h without plasma separation and for 6 h after separation at 4 °C resulted in coefficients of variations (CV) for hydroxy-PUFA being 10% higher than the respective analytical variance determined from the variance of the quality control plasma (Fig. S9) and storage for 1 h or 6 h at 4 °C increased the CV of epoxy-PUFA. Of note, the increased variances of the epoxy-PUFA might also be due to

possible artificial formation of epoxy-PUFAs during sample preparation using a silica based solid phase extraction material [32]. Additionally, vortexing of samples (simulating hemolysis) increased the CV of many oxylipins. Interestingly, it seems that autoxidative processes do not contribute to increased variances (except for the worst case scenario) since the CV of the isoprostane 5(*R*,*S*)-F_{2t}-IsoP did not change. The higher variation with no change in the relative concentrations compelled us to conclude that the blood of the participants is differently affected by storage (Fig. S9, Table S6) [1]. This emphasizes the importance of a standardized method for plasma generation, storage and preparation to ensure a good comparability in clinical studies.

Oxylipin stability during long-term storage at -80°C. Biological samples such as human plasma are usually stored at −80 °C until analysis to minimize artificial alteration of the oxylipin profile. In longitudinal studies with large cohorts, plasma samples are generated at different time points and thus are often stored for years before analysis. Hence, the storage stability of oxylipins is crucial for the comparability and validity of such studies. Indeed, basically almost all oxylipins were stable and the observed changes in the concentrations were within the analytical variance of ± 20–30% (Fig. 4, Table 2, Fig. S10) which is in line with our previous observation on the stability of free oxylipins [1]. Autoxidatively rather than enzymatically formed products seem to be relevantly affected when plasma samples are stored for longer time periods at −80 °C. The concentration of 9-HETE exceeded the analytical variance over the span of 15 months probably due to peroxidation wherein first a hydroperoxide is formed which is subsequently reduced to the corresponding hydroxy-PUFA [60,61]. Interestingly, oxylipins whose concentrations showed a slight decreasing trend over time are mainly CYP-derived or CYP-derived secondary products like vicinal dihydroxy-PUFA (Fig. 4, Table 2, Table S7). However, the change was within the analytical variance, thus indicating that epoxy-PUFA, which are of high interest in biological studies due to their pronounced physiological activity, remain stable and were not hydrolyzed (non)enzymatically to their respective dihydroxy-PUFA in stored plasma.

In other long-term studies investigating the influence of storage on the pattern of mainly free oxylipins contradictory results were observed [26,27]. The storage of plasma at −80 °C for 6 months resulted in decreased levels of most eicosanoids [26] whereas storing of plasma at −80 °C for one year led to increased levels of hydroxy-PUFA and TxB_2 [27]. Barden et al. reported elevated levels of total (i.e. free and esterified) F_2-isoprostanes after 6 months of storage at −80 °C [62]. These findings which are different from our results might be again explained by the generation and the quality, i.e. its initial peroxide content, of the used plasma. Nevertheless, our results indicate that storage of plasma samples at −80 °C is suitable for total oxylipin analysis. This aspect of stability of oxylipins in properly stored plasma samples is another key point regarding their potential use as biomarkers in health and disease.

5. Conclusion

In our study we investigated the influence of different additives during sample preparation and the impact of the transitory stage during plasma generation as well as the effects of long-term storage of plasma on the pattern of total oxylipins in human plasma.

Our results demonstrate that the use of the antioxidant BHT reduced the artificial formation of hydroxy-PUFA highlighting the importance of standardized analytical methods for reliable and reproducible quantification of total oxylipins.

The levels of total oxylipins in plasma are stable during the transitory stage of plasma generation. Significant differences in the concentrations result only when delays occur in all steps, namely centrifugation of whole blood, plasma separation as well as freezing of the plasma. Storage of plasma at −80 °C for 15 months slightly increased autoxidatively formed products.

Overall, our results indicate that the total oxylipin pattern is – if antioxidants are used during sample preparation – robust towards minor variations in plasma generation and long-term storage. As a consequence, it is possible to investigate the total oxylipin pattern in clinical samples and in prospective cohorts. Thus, using a targeted metabolomics approach as described here allows to generate biologically meaningful oxylipin pattern which can pave the route towards a mechanistical understanding of oxylipin biology and their role as biomarkers in diseases.

Declaration of competing interest

The authors declare no conflict of interest.

Acknowledgements

This study was supported by a grant (01EA1702) of the German Federal Ministry for Education and Research (BMBF) to NHS in the framework of the European Joint Programming Initiative “A Healthy Diet for a Healthy Life” (JPI HDHL; http://www.healthydietforhealthylife.eu/) to NHS, CG and JBM.

Appendix A. Supplementary data

Supplementary data to this article can be found online at https://doi.org/10.1016/j.talanta.2020.121074.

References

[1] C. Gladine, A.I. Ostermann, J.W. Newman, N.H. Schebb, MS-based targeted metabolomics of eicosanoids and other oxylipins: analytical and inter-individual variabilities, Free Radic. Biol. Med. 144 (2019) 72–89.
[2] M. Gabbs, S. Leng, J.G. Devassy, M. Monirujjaman, H.M. Aukema, Advances in our understanding of oxylipins derived from dietary PUFAs, Adv. Nutr. 6 (5) (2015) 513–540.
[3] M.W. Buczynski, D.S. Dumlao, E.A. Dennis, An integrated omics analysis of eicosanoid biology (vol 50, pg 1015, 2009), J. Lipid Res. 50 (7) (2009) 1505-1505.
[4] C.D. Funk, Prostaglandins and leukotrienes: advances in eicosanoid biology, Science 294 (5548) (2001) 1871–1875.
[5] C.N. Serhan, Pro-resolving lipid mediators are leads for resolution physiology, Nature 510 (7503) (2014) 92–101.
[6] C. Arnold, M. Markovic, K. Blossey, G. Wallukat, R. Fischer, R. Dechend, A. Konkel, C. von Schacky, F.C. Luft, D.N. Muller, M. Rothe, W.H. Schunck, Arachidonic acid-metabolizing cytochrome P450 enzymes are targets of omega-3 fatty acids, J. Biol. Chem. 285 (43) (2010) 32720–32733.
[7] C. Morisseau, B.D. Hammock, Impact of soluble epoxide hydrolase and epoxyeicosanoids on human health, Annu. Rev. Pharmacol. Toxicol. 53 (2013) 37–58.
[8] G.L. Milne, Q. Dai, L.J. Roberts, 2nd, the isoprostanes–25 years later, Biochim. Biophys. Acta 1851 (4) (2015) 433–445.
[9] H. Yin, L. Xu, N.A. Porter, Free radical lipid peroxidation: mechanisms and analysis, Chem. Rev. 111 (10) (2011) 5944–5972.
[10] D.F. Legler, M. Bruckner, E. Uetz-von Allmen, P. Krause, Prostaglandin E2 at new glance: novel insights in functional diversity offer therapeutic chances, Int. J. Biochem. Cell Biol. 42 (2) (2010) 198–201.
[11] D.L. Simmons, R.M. Botting, T. Hla, Cyclooxygenase isozymes: the biology of prostaglandin synthesis and inhibition, Pharmacol. Rev. 56 (3) (2004) 387–437.
[12] W. Wang, J. Zhu, F. Lyu, D. Panigrahy, K.W. Ferrara, B. Hammock, G. Zhang, omega-3 polyunsaturated fatty acids-derived lipid metabolites on angiogenesis, inflammation and cancer, Prostag. Other Lipid Mediat. 113–115 (2014) 13–20.
[13] G.D. Zhang, D. Panigrahy, L.M. Mahakian, J. Yang, J.Y. Liu, K.S.S. Lee, H.I. Wettersten, A. Ulu, X.W. Hu, S. Tam, S.H. Hwang, E.S. Ingham, M.W. Kieran, R.H. Weiss, K.W. Ferrara, B.D. Hammock, Epoxy metabolites of docosahexaenoic acid (DHA) inhibit angiogenesis, tumor growth, and metastasis, Proc. Natl. Acad. Sci. U.S.A. 110 (16) (2013) 6530–6535.
[14] C. Morin, M. Sirois, V. Echave, R. Albadine, E. Rousseau, 17,18-Epoxyeicosatetraenoic acid targets PPAR gamma and p38 mitogen-activated protein kinase to mediate its anti-inflammatory effects in the lung, Am. J. Resp. Cell. Mol. 43 (5) (2010) 564–575.
[15] L. Kutzner, K. Goloshchapova, D. Heydeck, S. Stehling, H. Kuhn, N.H. Schebb, Mammalian ALOX15 orthologs exhibit pronounced dual positional specificity with docosahexaenoic acid, Biochim. Biophys. Acta Mol. Cell Biol. Lipids 1862 (7) (2017) 666–675.
[16] J.P. Schuchardt, A.I. Ostermann, L. Stork, L. Kutzner, H. Kohrs, T. Greupner, A. Hahn, N.H. Schebb, Effects of docosahexaenoic acid supplementation on PUFA levels in red blood cells and plasma, Prostaglandins Leukot. Essent. Fatty Acids 115 (2016) 12–23.
[17] A.I. Ostermann, A.L. West, K. Schoenfeld, L.M. Browning, C.G. Walker, S.A. Jebb, P.C. Calder, N.H. Schebb, Plasma oxylipins respond in a linear dose-response

manner with increased intake of EPA and DHA: results from a randomized controlled trial in healthy humans, Am. J. Clin. Nutr. 109 (5) (2019) 1251–1263.
[18] A.I. Ostermann, N.H. Schebb, Effects of omega-3 fatty acid supplementation on the pattern of oxylipins: a short review about the modulation of hydroxy-, dihydroxy-, and epoxy-fatty acids, Food Funct. 8 (7) (2017) 2355–2367.
[19] M.L. Nording, J. Yang, K. Georgi, C. Hegedus Karbowski, J.B. German, R.H. Weiss, R.J. Hogg, J. Trygg, B.D. Hammock, A.M. Zivkovic, Individual variation in lipidomic profiles of healthy subjects in response to omega-3 Fatty acids, PloS One 8 (10) (2013) e76575.
[20] K. Brune, P. Patrignani, New insights into the use of currently available non-steroidal anti-inflammatory drugs, J. Pain Res. 8 (2015) 105–118.
[21] M. Steuck, S. Hellhake, N.H. Schebb, Food polyphenol apigenin inhibits the cytochrome P450 monoxygenase branch of the arachidonic acid cascade, J. Agric. Food Chem. 64 (47) (2016) 8973–8976.
[22] I. Willenberg, A.I. Ostermann, N.H. Schebb, Targeted metabolomics of the arachidonic acid cascade: current state and challenges of LC-MS analysis of oxylipins, Anal. Bioanal. Chem. 407 (10) (2015) 2675–2683.
[23] P.J. Taylor, Matrix effects: the Achilles heel of quantitative high-performance liquid chromatography-electrospray-tandem mass spectrometry, Clin. Biochem. 38 (4) (2005) 328–334.
[24] B.K. Matuszewski, M.L. Constanzer, C.M. Chavez-Eng, Matrix effect in quantitative LC/MS/MS analyses of biological fluids: a method for determination of finasteride in human plasma at picogram per milliliter concentrations, Anal. Chem. 70 (5) (1998) 882–889.
[25] A.I. Ostermann, I. Willenberg, K.H. Weylandt, N.H. Schebb, Development of an online-SPE-LC-MS/MS method for 26 hydroxylated polyunsaturated fatty acids as rapid targeted metabolomics approach for the LOX, CYP, and autoxidation pathways of the arachidonic acid cascade, Chromatographia 78 (5–6) (2015) 415–428.
[26] J. Dorow, S. Becker, L. Kortz, J. Thiery, S. Hauschildt, U. Ceglarek, Preanalytical investigation of polyunsaturated fatty acids and eicosanoids in human plasma by liquid chromatography-tandem mass spectrometry, Biopreserv. Biobanking 14 (2) (2016) 107–113.
[27] H.S. Jonasdottir, H. Brouwers, R.E.M. Toes, A. Ioan-Facsinay, M. Giera, Effects of anticoagulants and storage conditions on clinical oxylipid levels in human plasma, Biochim. Biophys. Acta Mol. Cell Biol. Lipids 1863 (12) (2018) 1511–1522.
[28] N.H. Schebb, A.I. Ostermann, J. Yang, B.D. Hammock, A. Hahn, J.P. Schuchardt, Comparison of the effects of long-chain omega-3 fatty acid supplementation on plasma levels of free and esterified oxylipins, Prostag. Other Lipid Mediat. 113 (2014) 21–29.
[29] J.D. Morrow, J.A. Awad, H.J. Boss, I.A. Blair, L.J. Roberts, 2nd, Non-cyclooxygenase-derived prostanoids (F2-isoprostanes) are formed in situ on phospholipids, Proc. Natl. Acad. Sci. U. S. A. 89 (22) (1992) 10721–10725.
[30] N.M. Hartung, M. Mainka, N. Kampschulte, A.I. Ostermann, N.H. Schebb, A strategy for validating concentrations of oxylipin standards for external calibration, Prostag. Other Lipid Mediat. 141 (2019) 22–24.
[31] E.M. Agency, Guideline on Bioanalytical Method Validation, (2011) EMEA/CHMP/EWP/192217/2009 Rev. 1 Corr. 2.
[32] A.I. Ostermann, E. Koch, K.M. Rund, L. Kutzner, M. Mainka, N.H. Schebb, Targeting Esterified Oxylipin by LC-MS - Effect of Sample Preparation on Oxylipin Pattern, Prostaglandins & Other Lipid Mediators, 2019.
[33] K.M. Rund, A.I. Ostermann, L. Kutzner, J.M. Galano, C. Oger, C. Vigor, S. Wecklein, N. Seiwert, T. Durand, N.H. Schebb, Development of an LC-ESI(-)-MS/MS method for the simultaneous quantification of 35 isoprostanes and isofurans derived from the major n3- and n6-PUFAs, Anal. Chim. Acta 1037 (2018) 63–74.
[34] L. Kutzner, K.M. Rund, A.I. Ostermann, N.M. Hartung, J.M. Galano, L. Balas, T. Durand, M.S. Balzer, S. David, N.H. Schebb, Development of an optimized LC-MS method for the detection of specialized pro-resolving mediators in biological samples, Front. Pharmacol. 10 (2019) 169.
[35] A.I. Ostermann, T. Greupner, L. Kutzner, N.M. Hartung, A. Hahn, J.P. Schuchardt, N.H. Schebb, Intra-individual variance of the human plasma oxylipin pattern: low inter-day variability in fasting blood samples versus high variability during the day, Anal. Meth. UK 10 (40) (2018) 4935–4944.
[36] G.C. Shearer, J.W. Newman, Impact of circulating esterified eicosanoids and other oxylipins on endothelial function, Curr. Atherosclerosis Rep. 11 (6) (2009) 403–410.
[37] D. Fulton, J.R. Falck, J.C. McGiff, M.A. Carroll, J. Quilley, A method for the determination of 5,6-EET using the lactone as an intermediate in the formation of the diol, J. Lipid Res. 39 (8) (1998) 1713–1721.
[38] G. Carlin, Peroxidation of linolenic acid promoted by human polymorphonuclear leucocytes, J. Free Radic. Biol. Med. 1 (4) (1985) 255–261.
[39] J. Yang, K. Schmelzer, K. Georgi, B.D. Hammock, Quantitative profiling method for oxylipin metabolome by liquid chromatography electrospray ionization tandem mass spectrometry, Anal. Chem. 81 (19) (2009) 8085–8093.
[40] N.A. Porter, L.S. Lehman, B.A. Weber, K.J. Smith, Unified mechanism for polyunsaturated fatty-acid autoxidation - competition of peroxy radical hydrogen-atom abstraction, beta-scission, and cyclization, J. Am. Chem. Soc. 103 (21) (1981) 6447–6455.
[41] H. Yin, J.D. Brooks, L. Gao, N.A. Porter, J.D. Morrow, Identification of novel autoxidation products of the omega-3 fatty acid eicosapentaenoic acid in vitro and in vivo, J. Biol. Chem. 282 (41) (2007) 29890–29901.
[42] M. Ouellet, M.D. Percival, Effect of inhibitor time-dependency on selectivity towards cyclooxygenase isoforms, Biochem. J. 306 (Pt 1) (1995) 247–251.
[43] S.H. Hwang, H.J. Tsai, J.Y. Liu, C. Morisseau, B.D. Hammock, Orally bioavailable potent soluble epoxide hydrolase inhibitors, J. Med. Chem. 50 (16) (2007) 3825–3840.
[44] T.R. Harris, B.D. Hammock, Soluble epoxide hydrolase: gene structure, expression and deletion, Gene 526 (2) (2013) 61–74.
[45] J.M. Braughler, L.A. Duncan, R.L. Chase, The involvement of iron in lipid peroxidation. Importance of ferric to ferrous ratios in initiation, J. Biol. Chem. 261 (22) (1986) 10282–10289.
[46] G. Astarita, A.C. Kendall, E.A. Dennis, A. Nicolaou, Targeted lipidomic strategies for oxygenated metabolites of polyunsaturated fatty acids, Biochim. Biophys. Acta 1851 (4) (2015) 456–468.
[47] N.M. Hartung, J. Fischer, A.I. Ostermann, I. Willenberg, K.M. Rund, N.H. Schebb, U. Garscha, Impact of food polyphenols on oxylipin biosynthesis in human neutrophils, Biochim. Biophys. Acta Mol. Cell Biol. Lipids 1864 (10) (2019) 1536–1544.
[48] J.Z. Haeggstrom, C.D. Funk, Lipoxygenase and leukotriene pathways: biochemistry, biology, and roles in disease, Chem. Rev. 111 (10) (2011) 5866–5898.
[49] J.M. Young, S. Panah, C. Satchawatcharaphong, P.S. Cheung, Human whole blood assays for inhibition of prostaglandin G/H synthases-1 and -2 using A23187 and lipopolysaccharide stimulation of thromboxane B2 production, Inflamm. Res. 45 (5) (1996) 246–253.
[50] C. Mesaros, I.A. Blair, Targeted chiral analysis of bioactive arachidonic Acid metabolites using liquid-chromatography-mass spectrometry, Metabolites 2 (2) (2012) 337–365.
[51] K. Keeren, D. Huang, C. Smyl, A. Fischer, M. Rothe, K.H. Weylandt, Effect of different omega-6/omega-3 polyunsaturated fatty acid ratios on the formation of monohydroxylated fatty acids in THP-1 derived macrophages, Biology (Basel) 4 (2) (2015) 314–326.
[52] C. Brideau, S. Kargman, S. Liu, A.L. Dallob, E.W. Ehrich, I.W. Rodger, C.C. Chan, A human whole blood assay for clinical evaluation of biochemical efficacy of cyclooxygenase inhibitors, Inflamm. Res. 45 (2) (1996) 68–74.
[53] M. Cattaneo, A. Lecchi, M.L. Zighetti, F. Lussana, Platelet aggregation studies: autologous platelet-poor plasma inhibits platelet aggregation when added to platelet-rich plasma to normalize platelet count, Haematologica 92 (5) (2007) 694–697.
[54] A.C. Soderstrom, M. Nybo, C. Nielsen, P.J. Vinholt, The effect of centrifugation speed and time on pre-analytical platelet activation, Clin. Chem. Lab. Med. 54 (12) (2016) 1913–1920.
[55] B. Kamlage, S.G. Maldonado, B. Bethan, E. Peter, O. Schmitz, V. Liebenberg, P. Schatz, Quality markers addressing preanalytical variations of blood and plasma processing identified by broad and targeted metabolite profiling, Clin. Chem. 60 (2) (2014) 399–412.
[56] V.B. O'Donnell, R.C. Murphy, S.P. Watson, Platelet lipidomics: modern day perspective on lipid discovery and characterization in platelets, Circ. Res. 114 (7) (2014) 1185–1203.
[57] G. Lippi, N. Blanckaert, P. Bonini, S. Green, S. Kitchen, V. Palicka, A.J. Vassault, M. Plebani, Haemolysis: an overview of the leading cause of unsuitable specimens in clinical laboratories, Clin. Chem. Lab. Med. 46 (6) (2008) 764–772.
[58] C.E. Ramsden, Z.X. Yuan, M.S. Horowitz, D. Zamora, S.F. Majchrzak-Hong, B.S. Muhlhausler, A.Y. Taha, M. Makrides, R.A. Gibson, Temperature and time-dependent effects of delayed blood processing on oxylipin concentrations in human plasma, Prostaglandins Leukot. Essent. Fatty Acids 150 (2019) 31–37.
[59] A.I. Ostermann, I. Willenberg, N.H. Schebb, Comparison of sample preparation methods for the quantitative analysis of eicosanoids and other oxylipins in plasma by means of LC-MS/MS, Anal. Bioanal. Chem. 407 (5) (2015) 1403–1414.
[60] Z. Mallat, T. Nakamura, J. Ohan, G. Leseche, A. Tedgui, J. Maclouf, R.C. Murphy, The relationship of hydroxyeicosatetraenoic acids and F-2-isoprostanes to plaque instability in human carotid atherosclerosis, J. Clin. Invest. 103 (3) (1999) 421–427.
[61] D.M. Guido, R. Mckenna, W.R. Mathews, Quantitation of hydroperoxy-eicosatetraenoic acids and hydroxy-eicosatetraenoic acids as indicators of lipid-peroxidation using gas-chromatography mass-spectrometry, Anal. Biochem. 209 (1) (1993) 123–129.
[62] A.E. Barden, E. Mas, K.D. Croft, M. Phillips, T.A. Mori, Minimizing artifactual elevation of lipid peroxidation products (F-2-isoprostanes) in plasma during collection and storage, Anal. Biochem. 449 (2014) 129–131.

Supplementary Information

Stability of oxylipins during plasma generation and long-term storage

Elisabeth Koch[*,1], Malwina Mainka[*,1], Céline Dalle[2], Annika I. Ostermann[1], Katharina M. Rund[1], Laura Kutzner[1], Laura-Fabienne Froehlich[1], Justine Bertrand-Michel[3], Cécile Gladine[2], Nils Helge Schebb[#,1]

[1]Chair of Food Chemistry, Faculty of Mathematics and Natural Sciences, University of Wuppertal, Wuppertal, Germany

[2]Université Clermont Auvergne, INRAe, UNH, Clermont-Ferrand, France

[3]MetaToul-MetaboHUB, Inserm/UPS UMR 1048 - I2MC, Institut des Maladies Métaboliques et Cardiovasculaires, Toulouse, France

[*]Authors contributed equally.

[#]Contact information for corresponding author:

Nils Helge Schebb
Chair of Food Chemistry
Faculty of Mathematics and Natural Sciences
University of Wuppertal
Gaußstr. 20
42119 Wuppertal
nils@schebb-web.de

Table of Contents

Preparation of oxylipin standard series

Oxylipins were combined to master mixes according to their molecular weight and sufficient chromatographic separation (Table S1). Master mixes were prepared in a volumetric flask (5 mL) with a tentative concentration of 10 µM based on the declaration of the manufacturer. Due to limited available standard material the regioisomers of EpODE and DiHODE, 9(10)-EpOME, 7(8)-EpDPE, 8,15-DiHETE, 5(*S*),6(*S*)-DiHETE, 8-HETE, 9-HETE and 11-HETE have been added at lower concentrations

The IS master was prepared in a volumetric flask (25 mL) with a tentative concentration of 5 µM. The internal standards $^{2}H_5$-RvD1 and $^{2}H_4$-PGB_2 were added at lower concentration because of their contamination with unlabeled isotopologs. The IS master was diluted with MeOH to a 100 nM "*sample preparation IS*"-solution in a volumetric flask and aliquoted in amber vials until use.

The purity and the concentration of the analytes in the master mixes was checked before pipetting the standard series (Figure S1).

All oxylipin solutions were prepared avoiding direct light radiation, using only detergent free glassware (no plastic) and stored at -80°C.

Determination of standard purity and verification of concentration

All master mixes were analyzed by means of LC-MS/MS in multiple reaction monitoring (MRM) mode. All transitions of not included analytes were evaluated for contamination/interferences. For detected interferences the standard compound containing the interference was identified. The contamination was quantified by calculating an area ratio between the contamination (at 5 µM) and the analyte standard at 5 µM. If an area ratio was higher than 10%, the contaminated oxylipin was removed from the standard series.

The master mixes were analyzed by means of LC-MS in single ion monitoring (SIM) mode and by means of UV spectroscopy according to Hartung *et al*., 2019 (Prostag Oth Lipid M 141, 22-24). The actual analyte concentration was adjusted by comparison with concentration-verified standard material.

Preparation of standard series

Calibrants with 16 concentrations levels were prepared by a sequential dilution with IS master (Table S2). The internal standards concentrations were 20 nM, except for $^{2}H_{5}$-RvD1 and $^{2}H_{4}$-PGB_{2} (5 nM and 10 nM in calibrants, respectively).

For calibration the peak area ratio (analyte/IS) was linearly fitted against the analyte concentration using linear least square regression (weighting $1/x^{2}$) (SI Table S3). The concentration with a signal to noise ratio of ≥3 was determined as limit of detection (LOD). The lower limit of quantification (LLOQ) was set to the concentration yielding a signal to noise ratio of ≥5 and accuracy of ± 20% within the calibration curve. The accuracy within the calibration curve was ± 15% fulfilling the validation criteria of the European Medicines Agency (EMA) guideline for bioanalyses (Agency, E. M. In *EMEA/CHMP/EWP/192217/2009 Rev. 1 Corr. 2*, 2011).

Sample preparation

To 100 µL thawed plasma 10 µL of IS solution (100 nM in MeOH) and 10 µL of antioxidant mixture (0.2 mg/mL BHT, 100 µM indomethacin, 100 µM trans-4-(-4-(3-adamantan-1-yl-ureido9-cyclohexyloxy)-benzoic acid (*t*-AUCB) in MeOH) were added. For protein precipitation 400 µL ice-cold *iso*-propanol was added and the samples were stored at -60°C for at least 30 min. Following centrifugation (4°C, 20000 x *g*, 10 min) the supernatant was collected and hydrolyzed at 60°C for 30 min using 100 µL of 0.6 M potassium hydroxide in MeOH/water (75/25; *v*/*v*). Afterwards samples were neutralized (pH=6) with acetic acid (HOAc), diluted with 2 mL of 0.1 M disodium hydrogen phosphate buffer (adjusted to pH 6 with HOAc) and loaded onto pre-conditioned SPE cartridges. The extraction of oxylipins with the anion exchange Bond Elut Certify II SPE cartridges (200 mg, 3 mL, Agilent, Waldbronn, Germany) was carried out as described in Rund *et al.* 2017 (Anal Chim Acta 1037, 63-74). Oxylipins were eluted with ethyl acetate/*n*-hexane (75/25, *v*/*v*) including 1% HOAc into a tube containing 6 µL of 30% glycerol in MeOH. After evaporation (vacuum concentrator, 30°C, 1 mbar; Christ, Osterode, Germany) the residue was reconstituted in 50 µL MeOH containing 40 nM of each, 1-(1-(ethylsulfonyl)piperidin-4-yl)-3-(4-(trifluoromethoxy)phenyl)urea, 12-(3-adamantan-1-yl-ureido)-dodecanoic acid, 12-oxo-phytodienoic acid and aleuritic acid, as IS2 to calculate the extraction efficiency of the deuterated IS.

Table S1: Composition of master mixes. Analytes are listed according to their molecular weight and retention time

molecular mass [Da]	precursor fatty acid	analyte	t_R [min]	Master								
				I (ALA/ LA II) *	II (LA/ ALA II) *	III (ARA)	IV (ARA II)	V (EPA) *	VI (DHA) *	VII (DHA/ EPA II) *	VIII (DGLA / ARA III)	IX (Div) *
266.4	ARA	tetranor-12-HETE	14.76			X						
280.4	ARA	12-HHTrE	15.64			X						
292.4	ALA	9-OxoOTrE	18.23	X								
	ALA	13-OxoOTrE	18.03		X							
294.4	ALA	9-HOTrE	16.89	X								
	ALA	13-HOTrE	17.25	X								
	LA	13-oxo-ODE	20.47		X							
	LA	9-oxo-ODE	20.75		X							
	GLA	13-γ-HOTrE	13.36									X
	ALA	9(10)-EpODE	20.03	X								
	ALA	12(13)-EpODE	20.48	X								
	ALA	15(16)-EpODE	19.86	X								
296.5	LA	9(10)-EpOME	22.49		X							
	LA	12(13)-EpOME	22.28		X							
	LA	9-HODE	19.37		X							
	LA	10-HODE	19.18									X
	LA	12-HODE	18.86		X							
	LA	13-HODE	19.26	X								
	LA	15-HODE	18.06		X							
298.5	Oleic	9(10)-Ep-stearic acid	24.03									X
312.5	ALA	9,10-DiHODE	12.74	X								
	ALA	12,13-DiHODE	12.85	X								
	ALA	15,16-DiHODE	12.68	X								
314.5	LA	9,10-DiHOME	14.92		X							
	LA	12,13-DiHOME	14.46		X							

Table S1: Continued

318.5	ARA	5-oxo-ETE	22.94								X	
	ARA	12-oxo-ETE	21.47								X	
	ARA	15-oxo-ETE	20.80								X	
	EPA	8(9)-EpETE	21.24					X				
	EPA	11(12)-EpETE	21.06							X		
	EPA	14(15)-EpETE	20.89					X				
	EPA	17(18)-EpETE	20.13					X				
	EPA	5-HEPE	19.06					X				
	EPA	8-HEPE	18.38							X		
	EPA	9-HEPE	18.73							X		
	EPA	11-HEPE	18.58					X				
	EPA	12-HEPE	18.17					X				
	EPA	15-HEPE	18.07							X		
	EPA	18-HEPE	17.34					X				
320.5	ARA	8(9)-EpETrE	23.25				X					
	ARA	11(12)-EpETrE	23.07			X						
	ARA	14(15)-EpETrE	22.50			X						
	ARA	5-HETE	21.62			X						
	ARA	8-HETE	20.97			X						
	ARA	9-HETE	21.35				X					
	ARA	11-HETE	20.57				X					
	ARA	12-HETE	21.02				X					
	ARA	15-HETE	20.02			X						
	ARA	16-HETE	18.77			X						
	ARA	17-HETE	18.61				X					
	ARA	18-HETE	18.37			X						
	ARA	19-HETE	17.78			X						
	ARA	20-HETE	18.03				X					

Table S1: Continued

322.5	DGLA	14(15)-EpEDE	23.62									X
	DGLA	5-HETrE	23.62								X	
	DGLA	8-HETrE	21.76								X	
	DGLA	12-HETrE	21.98									X
	DGLA	15-HETrE	21.43									X
326.4	ARA	2,3-dinor-15-(*R*,*S*)-15-F_{2t}-IsoP	5.14			X						
328.4	ALA	9,10,11-TriHODE	7.87	X								
	ALA	9,12,13-TriHODE	6.80		X							
	ALA	9,10,13-TriHODE	6.80	X								
330.5	LA	9,10,11-TriHOME	9.24		X							
	LA	9,12,13-TriHOME	7.87		X							
	LA	9,10,13-TriHOME	8.01		X							
332.4	EPA	PGB_3	10.02					X				
334.4	ARA	12-oxo LTB_4	14.82				X					
	ARA	PGJ_2	11.56				X					
	ARA	PGB_2	11.77			X						
	ARA	20-carboxy ARA	16.90				X					
336.5	ARA	8(*S*),15(*S*)-DiHETE	12.88			X						
	ARA	5(*S*),15(*S*)-DiHETE	13.32			X						
	ARA	5(*S*),12(*S*)-DiHETE	14.30			X						
	ARA	LTB_4	13.79				X					
	ARA	6-*trans*-LTB_4	13.30				X					
	ARA	5(*S*),6(*R*)-DiHETE	17.13								X	
	ARA	5(*S*),6(*S*)-DiHETE	18.00								X	
	ARA	6-*trans*-12-*epi* LTB_4	13.39								X	
	EPA	5,6-DiHETE	15.5					X				
	EPA	8,9-DiHETE	14.66					X				
	EPA	11,12-DiHETE	12.29					X				
	EPA	14,15-DiHETE	14.06					X				
	EPA	17,18-DiHETE	13.42					X				

Table S1: Continued

338.4	ARA	18-carboxy dinor LTB_4	4.32								X	
	ARA	5,6-DiHETrE	18.00				X					
	ARA	8,9-DiHETrE	17.11				X					
	ARA	11,12-DiHETrE	16.48				X					
	ARA	14,15-DiHETrE	15.69				X					
	DGLA	LTB_3	15.94								X	
342.5	DHA	4-oxo DHA	23.33							X		
	DHA	17-oxo DHA	21.07							X		
344.4	DHA	7(8)-EpDPE	23.18						X			
	DHA	10(11)-EpDPE	22.98							X		
	DHA	13(14)-EpDPE	22.87						X			
	DHA	16(17)-EpDPE	22.78							X		
	DHA	19(20)-EpDPE	22.29						X			
	DHA	4-HDHA	22.17							X		
	DHA	7-HDHA	21.25							X		
	DHA	8-HDHA	21.47						X			
	DHA	10-HDHA	20.78						X			
	DHA	11-HDHA	21.12									X
	DHA	13-HDHA	20.52						X			
	DHA	14-HDHA	20.79									X
	DHA	16-HDHA	20.21									X
	DHA	17-HDHA	20.35							X		
	DHA	20-HDHA	19.67						X			
	n3-DPA	17-oxo DPA	22.26									X
352.5	ARA	15-oxo-15-F_{2t}-IsoP	7.62			X						
	ARA	20-OH-LTB_4	6.10			X						
	ARA	LXA_4	9.74			X						
	EPA	$PGF_{3\alpha}$	6.88								X	
	EPA	15-F_{3t}-IsoP	5.94									X

Table S1: Continued

354.5	ARA	PGF_{2a}	8.08				X					
	ARA	15-F_{2t}-IsoP	7.33				X					
	ARA	13,14-dihydro-15-oxo-15-F_{2t}-IsoP	5.25								X	
	ARA	5(*R*,*S*)-5-F_{2t}-IsoP	7.57				X					
	ARA	5(*R*,*S*)-5-F_{2c}-IsoP	9.54				X					
356.5	DGLA	PGF_{1a}	8.13								X	
	DGLA	15-F_{1t}-IsoP	7.04								X	
360.5	DHA	RvD5	13.59							X		
	DHA	MaR2	15.09							X		
	DHA	PDx	13.51						X			
362.5	DHA	7,8-DiHDPE	17.84						X			
	DHA	10,11-DiHDPE	17.04						X			
	DHA	13,14-DiHDPE	16.67						X			
	DHA	16,17-DiHDPE	16.40						X			
	DHA	19,20-DiHDPE	15.76						X			
	n3-DPA	7(*S*),17(*S*)-diH DPA	14.06									X
366.5	ARA	20-COOH-LTB_4	5.87			X						
368.5	EPA	d17-6-keto-PGF_{1a}	5.17					X				
370.5	ARA	6-keto-PGF_{1a}	5.85			X						
376.5	DHA	RvD4	11.17						X			
382.5	AdA	1a,1b-dihomo-PGF_{2a}	10.63									X

*Isoprostanes and isofuranes may be added to the master mixes, as described in Rund *et al.*, 2017 Anal Chim Acta 1037, 63-74

Table S2: Pipetting scheme for the sequential dilution of the standard series

Calibrant number	Concentration level [nM]	final volume [mL]	Volume of standard [mL]	standard	Volume of IS Master [µL]	concentration IS [nM]
OXY 16	500	50	2.5	all Masters	200	20
OXY 15	250	20	10	OXY 16	40	20
OXY 14	100	50	10	OXY 16	160	20
OXY 13	50	50	5	OXY 16	180	20
OXY 12	25	25	2.5	OXY 15	90	20
OXY 11	10	50	5	OXY 14	180	20
OXY 10	5	50	5	OXY 13	180	20
OXY 9	2.5	25	2.5	OXY 12	90	20
OXY 8	1	25	2.5	OXY 11	90	20
OXY 7	0.75	20	1.5	OXY 11	74	20
OXY 6	0.5	25	2.5	OXY 10	90	20
OXY 5	0.25	25	2.5	OXY 9	90	20
OXY 4	0.1	25	2.5	OXY 8	90	20
OXY 3	0.05	20	2	OXY 6	72	20
OXY 2	0.025	20	2	OXY 5	72	20
OXY 1	0.01	20	2	OXY 4	72	20

Table S3: Parameters of the LC-ESI(-)-MS/MS method. Shown are transitions for each analyte for quantification in scheduled multiple reaction monitoring (MRM) mode, MS potentials (declustering potential (DP), entrance potential (EP), collision energy (CE), cell exit potential (CXP)), assigned internal standards (IS), retention time (t_R), full width at half maximum (FWHM), limit of detection (LOD), calibration range with lower limit of quantification (LLOQ) and upper limit of quantification (ULOQ), slope and correlation coefficient of the calibration curve (r^2).

1) full peak width at half maximum (FWHM) determined as mean width of standards (LLOQ - 500 nM)

2) limit of detection (LOD) set to lowest concentration with a signal to noise ratio ≥3

3) lower limit of quantification (LLOQ) set to lowest calibration standards with a signal to noise ratio ≥5 and accuracy ±20%

4) upper limit of quantification (ULOQ) set to calibration of the highest injected standard

5) calibration was performed as weighted regression using $1/x^2$ weighting

6) other isoprostanes, isofuranes and phytoprostanes can be included as described in Rund et al., 2017 (Anal Chim Acta 1037, 63-74)

Table S4: Statistical analysis of the effects of additives on the apparent oxylipin pattern. Statistical differences between "no additive" and different additives were evaluated by two-way ANOVA followed by Bonferroni post-test.

	anti-ox mix	BHT	EDTA	IND	t-AUCB
	p-val				
5-HETE	p <0.05	p <0.05	ns	ns	ns
9-HETE	p <0.01	p <0.01	ns	ns	ns
12-HETE	p <0.05	p <0.01	ns	ns	ns
15-HETE	p <0.001	p <0.001	ns	ns	ns
20-HETE	ns	ns	ns	ns	ns
5-HEPE	ns	p <0.05	ns	ns	ns
12-HEPE	p <0.01	p <0.01	ns	ns	ns
15-HEPE	p <0.05	p <0.001	ns	ns	ns
18-HEPE	p <0.001	p <0.001	ns	ns	ns
4-HDHA	p <0.001	p <0.001	ns	ns	ns
7-HDHA	ns	ns	ns	ns	ns
14-HDHA	p <0.01	p <0.01	ns	ns	ns
17-HDHA	p <0.001	p <0.001	ns	ns	ns
13-HODE	p <0.05	p <0.05	ns	ns	ns
13-HOTrE	ns	ns	ns	ns	ns
5(6)-EpETrE	ns	ns	ns	ns	ns
8(9)-EpETrE	ns	ns	ns	ns	ns
11(12)-EpETrE	ns	ns	ns	ns	ns
14(15)-EpETrE	ns	ns	ns	ns	ns
17(18)-EpETE	ns	p <0.05	ns	ns	ns
19(20)-EpDPE	ns	ns	ns	ns	ns
12(13)-EpOME	ns	ns	ns	ns	ns
15(16)-EpODE	ns	ns	ns	ns	ns
14,15-DiHETrE	ns	ns	ns	ns	ns
17,18-DiHETE	ns	ns	ns	ns	ns
19,20-DiHDPE	ns	ns	ns	ns	ns
12,13-DiHOME	ns	ns	ns	ns	ns
15,16-DiHODE	ns	ns	ns	ns	ns

Table S5: Oxylipin concentrations in quality standard (QS) plasma. Shown are analyzed oxylipins sorted by their retention time (t_R) with their mass transitions used for quantification in scheduled MRM mode, limit of detection (LOD) and calibration range with lower limit of quantification (LLOQ) and upper limit of quantification (ULOQ) in vial. For each analyte mean ± SD (n=8) concentration in plasma and ratio of determined concentration to LLOQ (fold LLOQ) was calculated. Plasma samples are concentrated during sample preparation by factor 2 yielding lower LLOQ in human plasma. The LLOQ is provided in grey when concentration of analyte was <LLOQ in more than 50% of the samples.

Table S6: Analyte concentrations of total oxylipins in human EDTA plasma during the transitory stage. Shown are mean ± SD concentrations for all storage conditions and times as well as for the QS plasma. Additionally, for each analyte lower limit of quantification (LLOQ) is displayed. When analyte concentration was <LLOQ in more than 50% of the samples the LLOQ (highlighted in grey) is shown instead of mean.

Table S7: Analyte concentrations of total oxylipins during long-term storage of human EDTA plasma. Shown are mean concentrations of oxylipins >LLOQ for all storage times. In addition, a concentration range of ±30% (corresponds to the analytical variance) was determined for each oxylipin based on the concentration quantified in month 1.

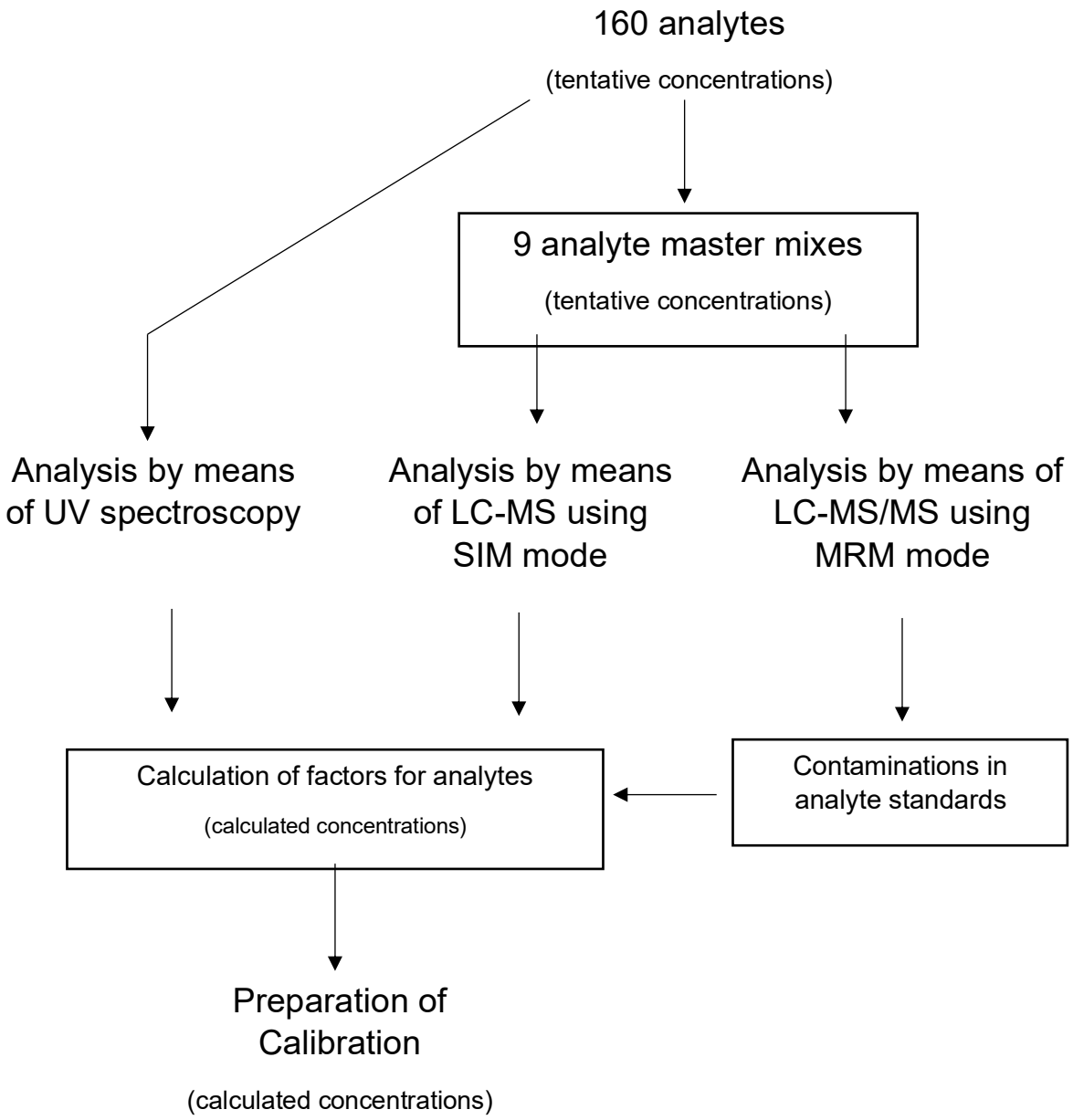

Figure S1: Scheme to generate an oxylipin multi-analyte standard series with characterized purity and concentration.

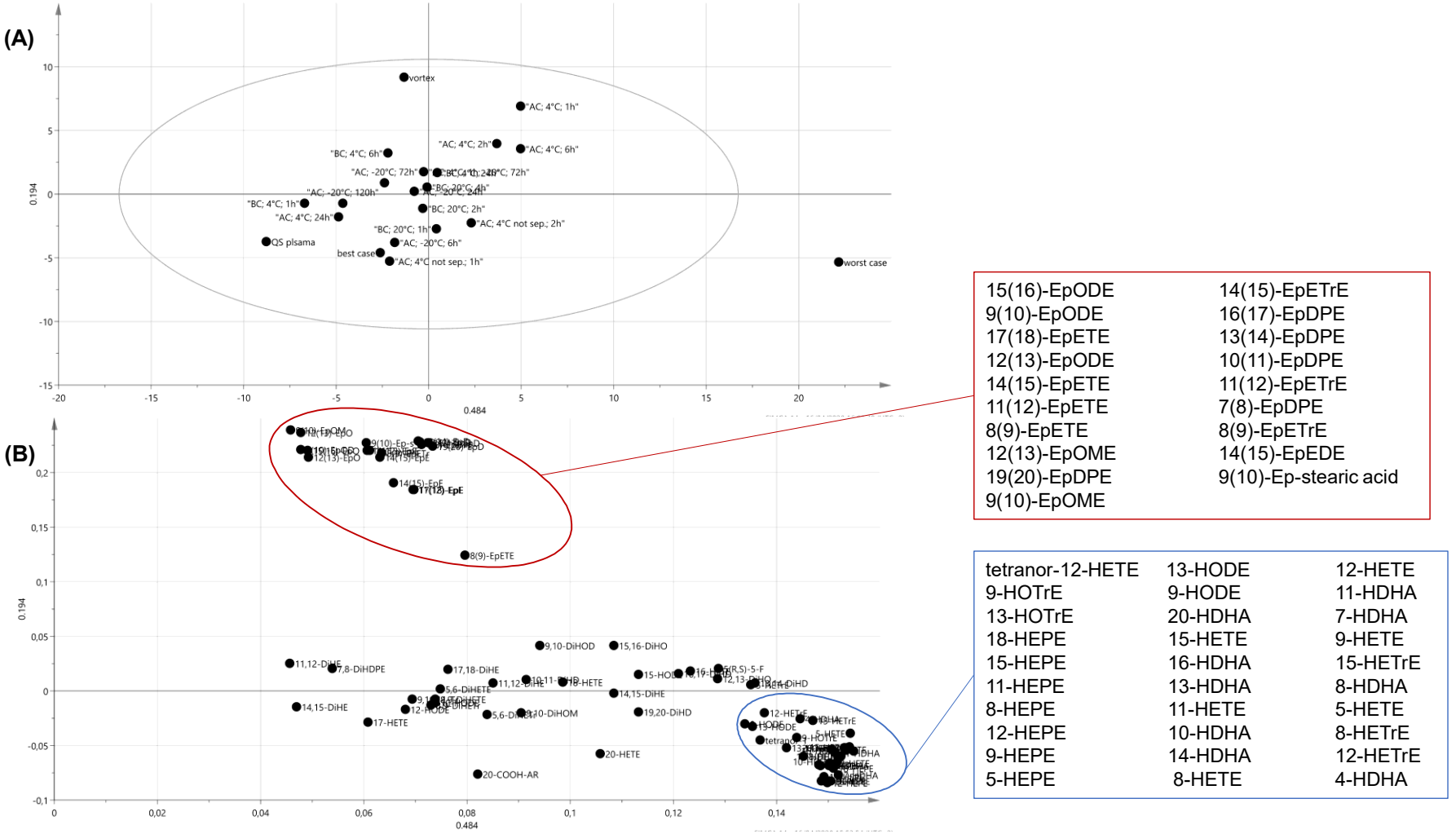

15(16)-EpODE	14(15)-EpETrE
9(10)-EpODE	16(17)-EpDPE
17(18)-EpETE	13(14)-EpDPE
12(13)-EpODE	10(11)-EpDPE
14(15)-EpETE	11(12)-EpETrE
11(12)-EpETE	7(8)-EpDPE
8(9)-EpETE	8(9)-EpETrE
12(13)-EpOME	14(15)-EpEDE
19(20)-EpDPE	9(10)-Ep-stearic acid
9(10)-EpOME	

tetranor-12-HETE	13-HODE	12-HETE
9-HOTrE	9-HODE	11-HDHA
13-HOTrE	20-HDHA	7-HDHA
18-HEPE	15-HETE	9-HETE
15-HEPE	16-HDHA	15-HETrE
11-HEPE	13-HDHA	8-HDHA
8-HEPE	11-HETE	5-HETE
12-HEPE	10-HDHA	8-HETrE
9-HEPE	14-HDHA	12-HETrE
5-HEPE	8-HETE	4-HDHA

Figure S2: Principal components analysis (PCA) model. A) The score plot for 1st (48% of variability) and 2nd (19% of variability) component shows the distribution of all storage conditions and identifies the worst case sample as main contributor to the variability. **B)** The loading plot shows to what extent the different storage conditions influence the oxylipin concentrations. “Vortex" influences the concentration of epoxy-PUFA (red box) and "worst case" has a great effect on the concentration of hydroxy-PUFA (blue box).

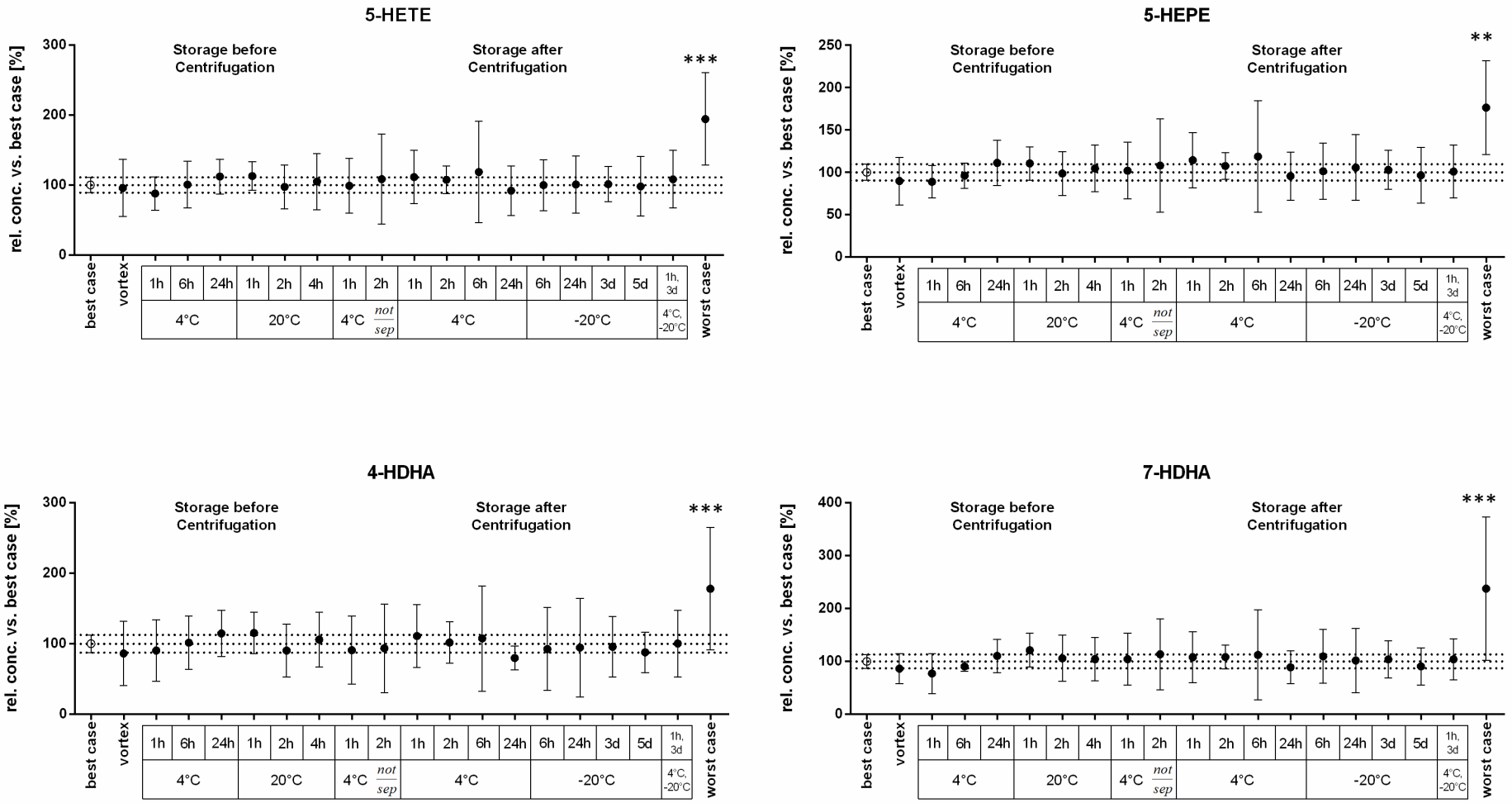

Figure S3: Concentrations of total oxylipins derived from 5-LOX pathway during the different storage conditions and times. The relative concentrations were calculated against the baseline concentration (best case sample). Shown are mean ± 95% CI (n=4; 12 for best case). The dotted lines mark the 95% CI of the best case sample. Statistical differences between baseline and different storage conditions were evaluated by one-way ANOVA followed by Tukey post-test (** p<0.01; *** p<0.001).

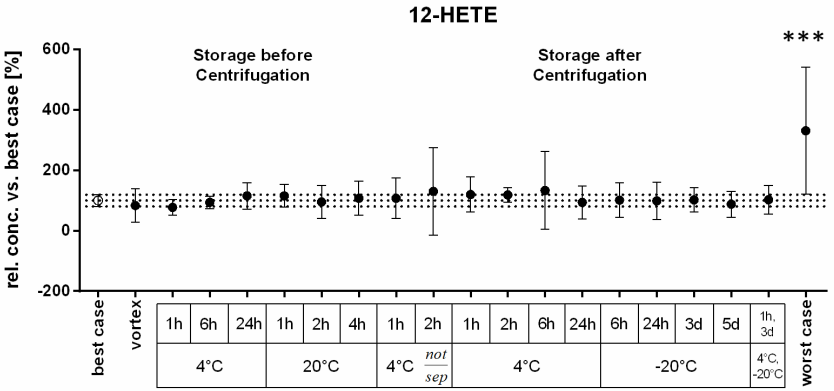

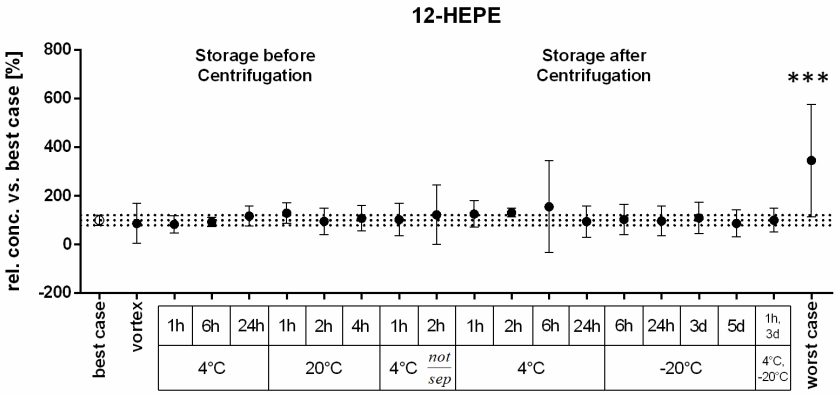

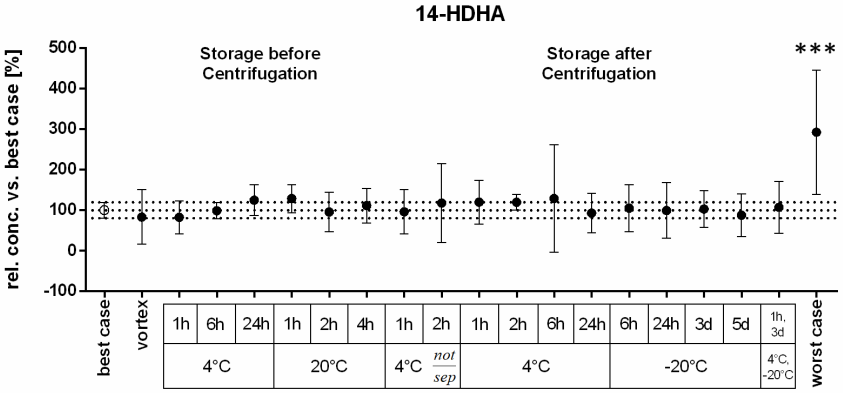

Figure S4: Concentrations of total oxylipins derived from 12-LOX pathway during the different storage conditions and times. The relative concentrations were calculated against the baseline concentration (best case sample). Shown are mean ± 95% CI (n=4, 12 for best case). The dotted lines mark the 95% CI of the best case sample. Statistical differences between baseline and different storage conditions were evaluated by one-way ANOVA followed by Tukey post-test (*** $p<0.001$).

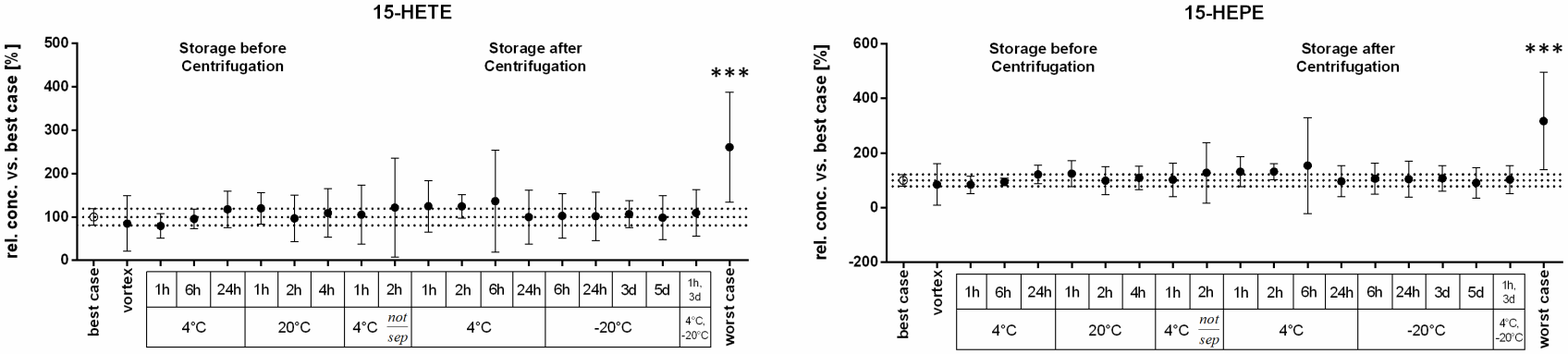

Figure S5: Concentrations of total oxylipins derived from 15-LOX pathway during the different storage conditions and times. The relative concentrations were calculated against the baseline concentration (best case sample). Shown are mean ± 95% CI (n=4; 12 for best case). The dotted lines mark the 95% CI of the best case sample. Statistical differences between baseline and different storage conditions were evaluated by one-way ANOVA followed by Tukey post-test (*** $p<0.001$). Of note, the detection of 17-HDHA was not possible due to high baseline.

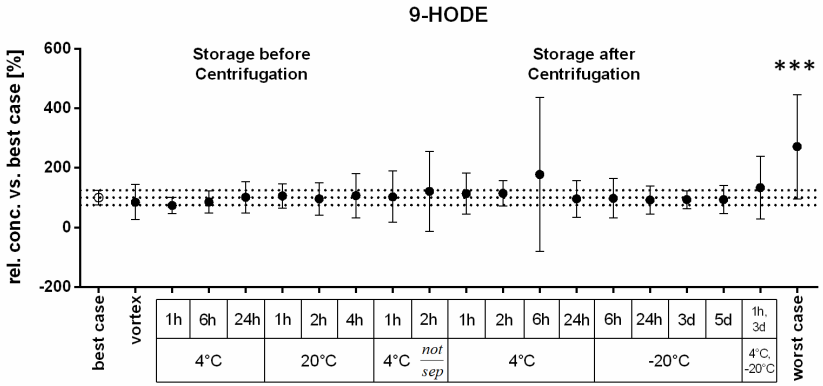

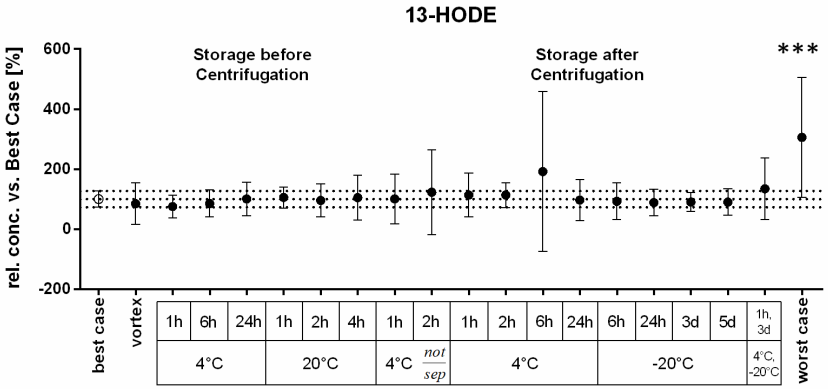

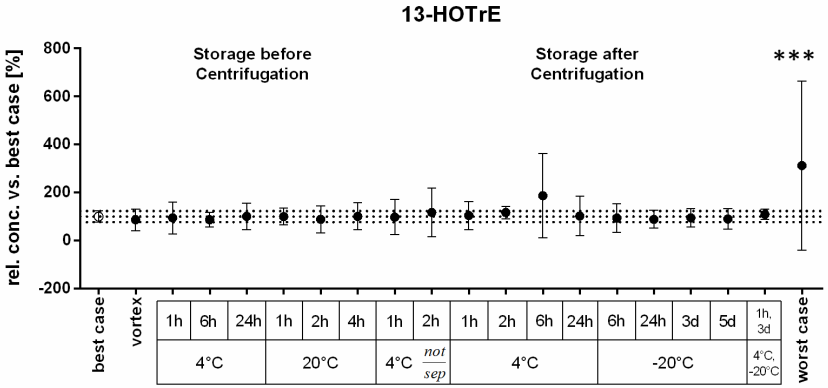

Figure S6: Concentrations of total hydroxy-PUFA derived from LA and ALA during the different storage conditions and times. The relative concentrations were calculated against the baseline concentration (best case sample). Shown are mean ± 95% CI (n=4; 12 for best case). The dotted lines mark the 95% CI of the best case sample. Statistical differences between baseline and different storage conditions were evaluated by one-way ANOVA followed by Tukey post-test (*** p<0.001).

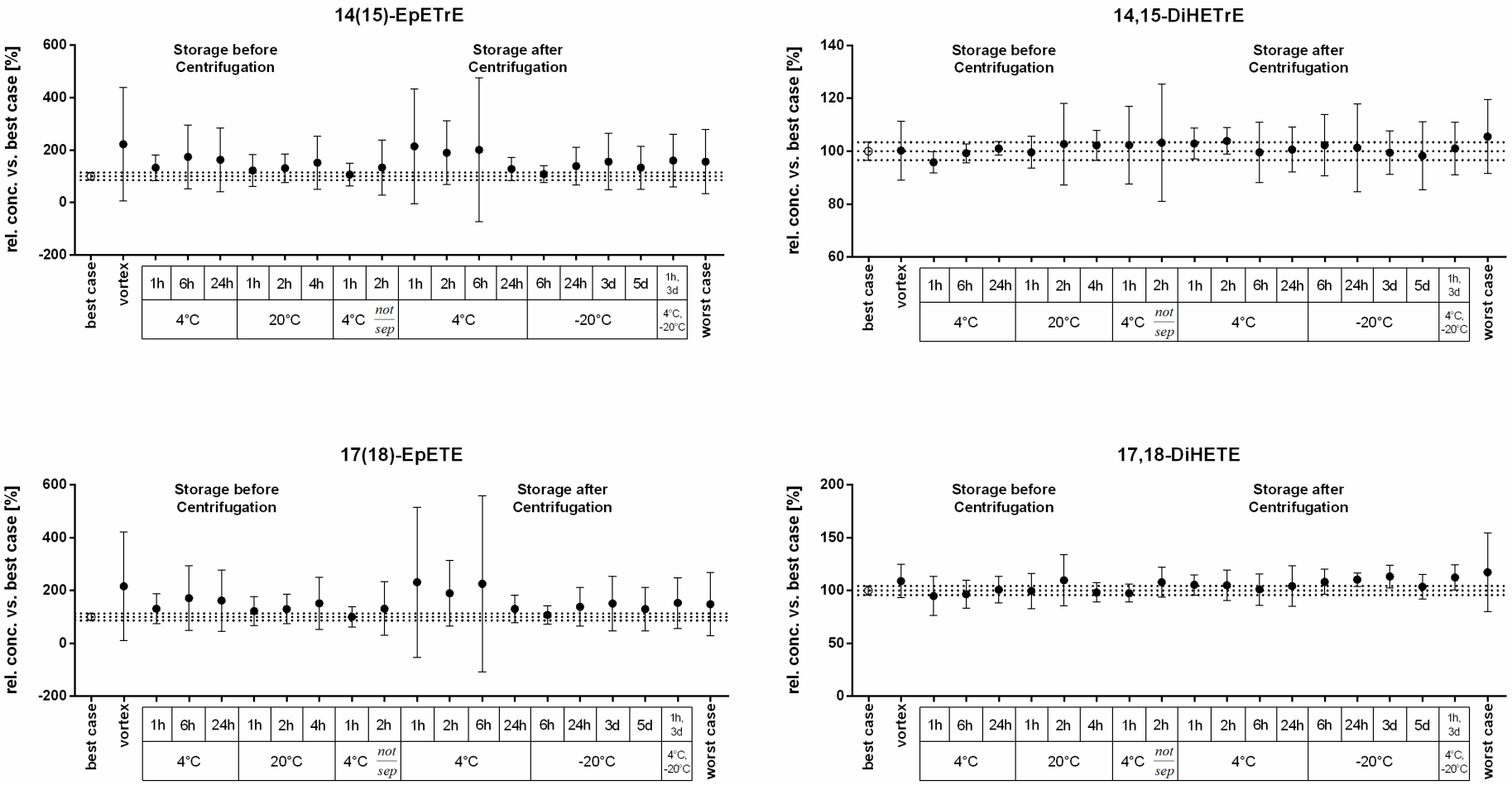

Figure S7: Concentrations of total oxylipins derived from CYP pathway during the different storage conditions and times. On the left Ep-PUFA are presented and on the right the respective s*EH* metabolites (DiH-PUFA). The relative concentrations were calculated against the baseline concentration (best case sample). Shown are mean ± 95% CI (n=4; 12 for best case). The dotted lines mark the 95% CI of the best case sample. Statistical differences between baseline and different storage conditions were evaluated by one-way ANOVA followed by Tukey post-test.

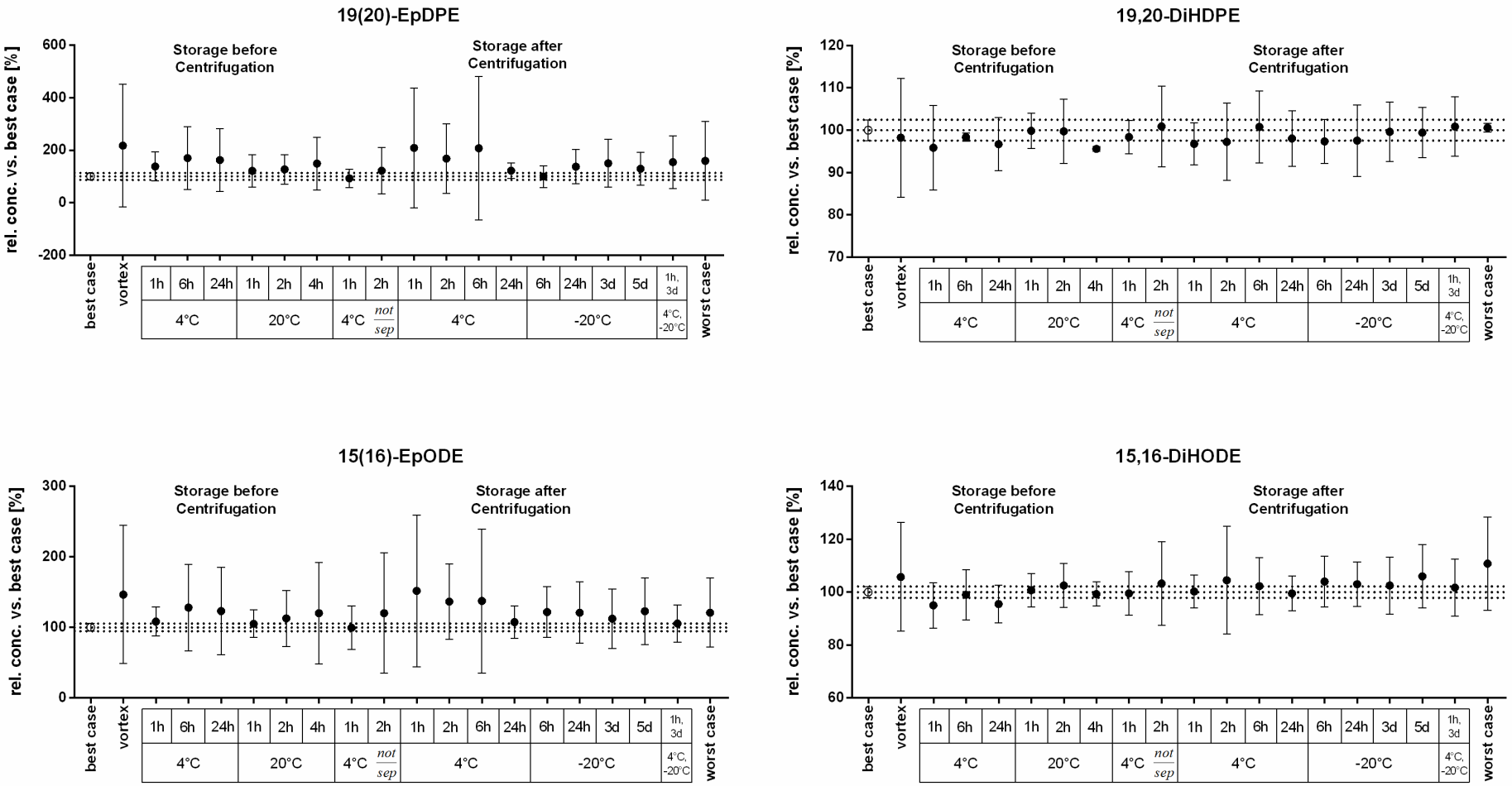

Figure S7: Continued

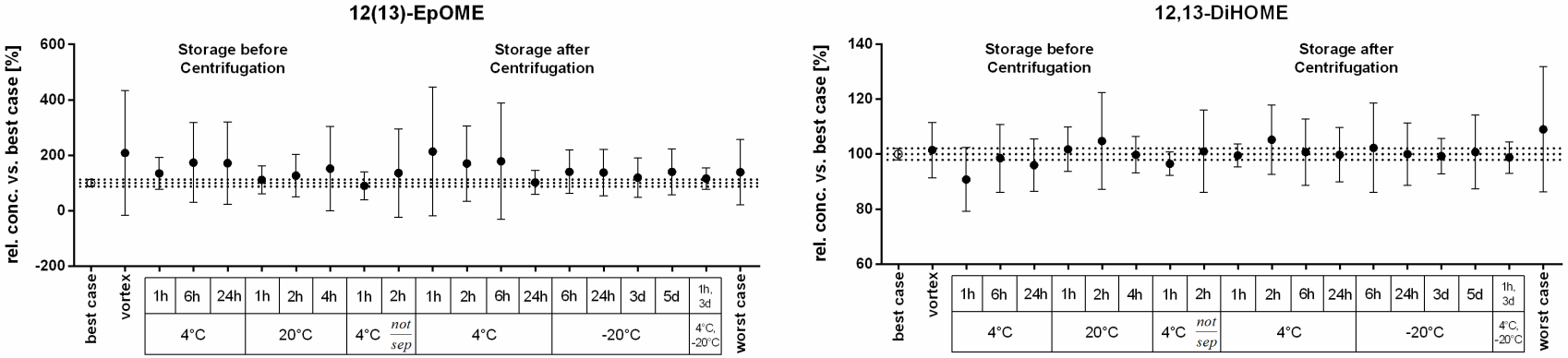

Figure S7: Continued

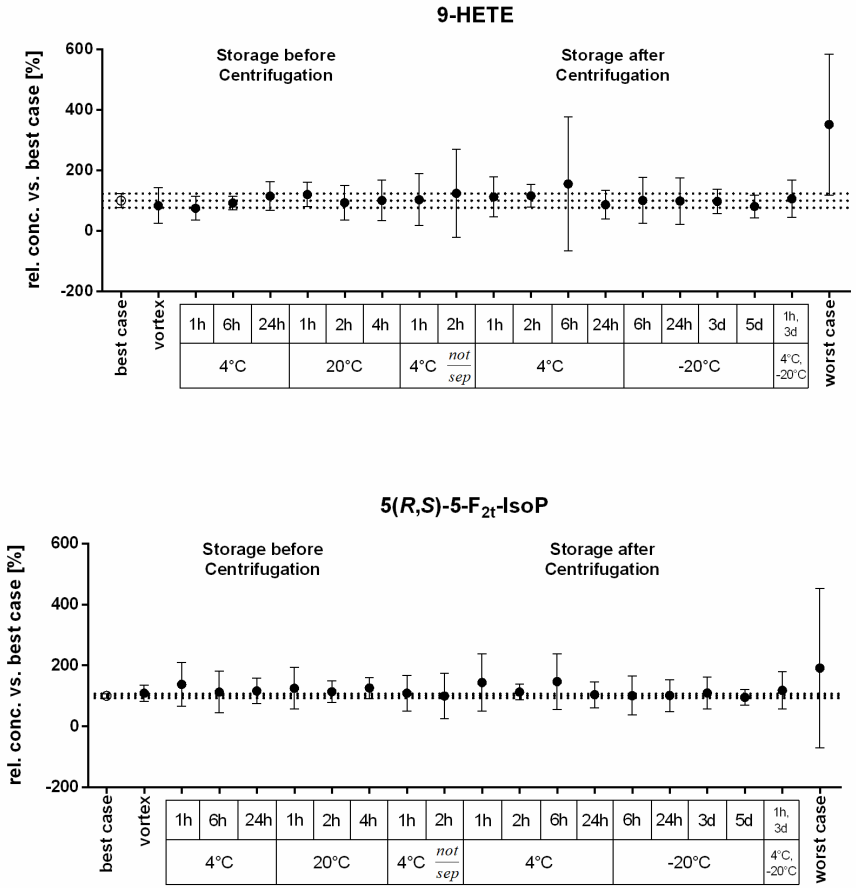

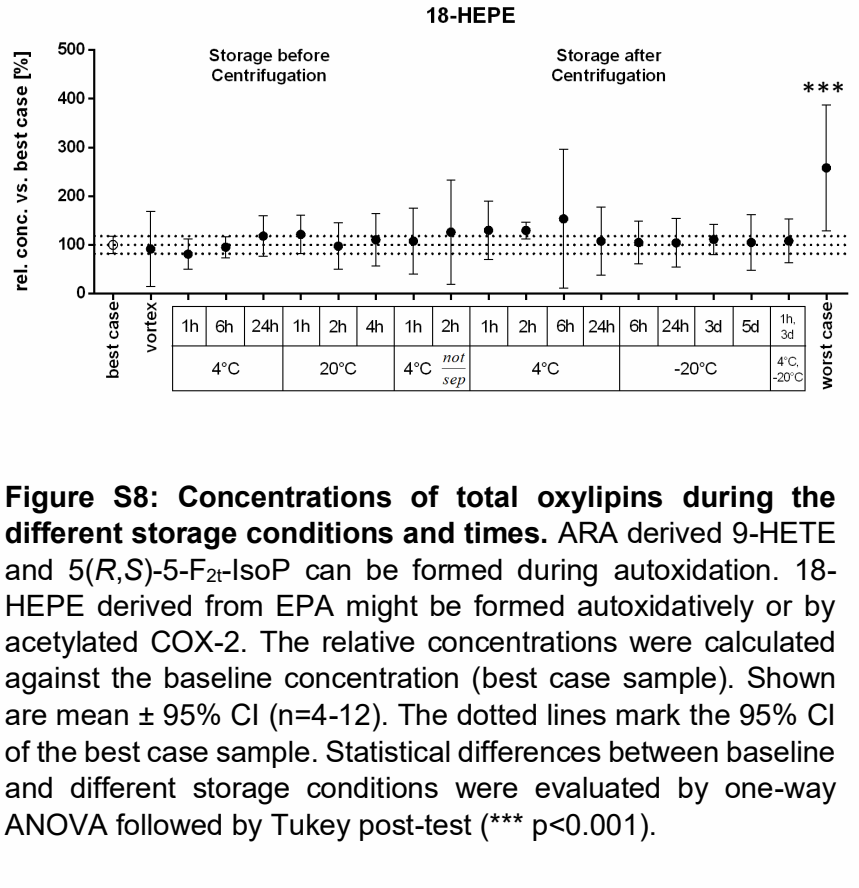

Figure S8: Concentrations of total oxylipins during the different storage conditions and times. ARA derived 9-HETE and 5(*R*,*S*)-5-F_{2t}-IsoP can be formed during autoxidation. 18-HEPE derived from EPA might be formed autoxidatively or by acetylated COX-2. The relative concentrations were calculated against the baseline concentration (best case sample). Shown are mean ± 95% CI (n=4-12). The dotted lines mark the 95% CI of the best case sample. Statistical differences between baseline and different storage conditions were evaluated by one-way ANOVA followed by Tukey post-test (*** p<0.001).

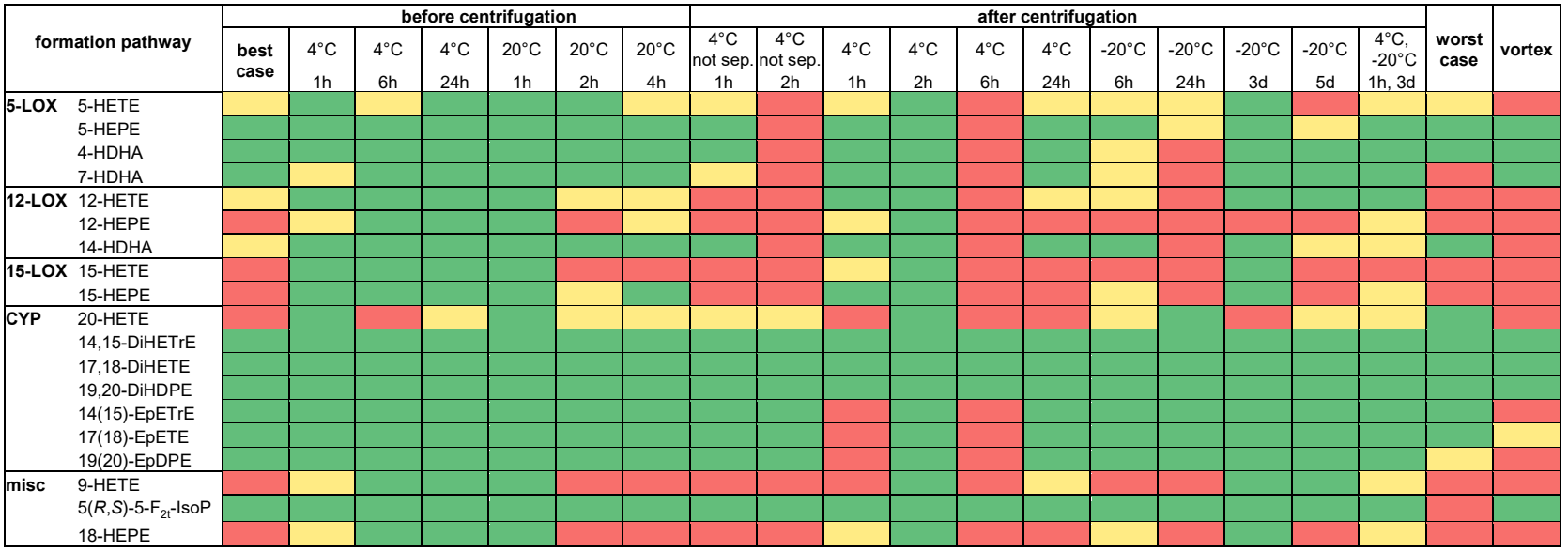

Figure S9: Effects of the different storage conditions on the coefficient of variance (CV). The CV ($\frac{SD}{mean} * 100$) of the differently stored samples was compared to the interbatch CV of quality standard (QS) plasma (2 batches on 4 days) (CV_{sample}-CV_{QS}). When the difference of the sample variance is lower than 5% (CV_{sample}<CV_{QS}+5%) the sample is highlighted in green. Differences between 5% and 10% (CV_{QS}+5%<CV_{sample}<CV_{QS}+10%) are marked in yellow and higher than 10 % (CV_{sample}>CV_{QS}+10%) in red.

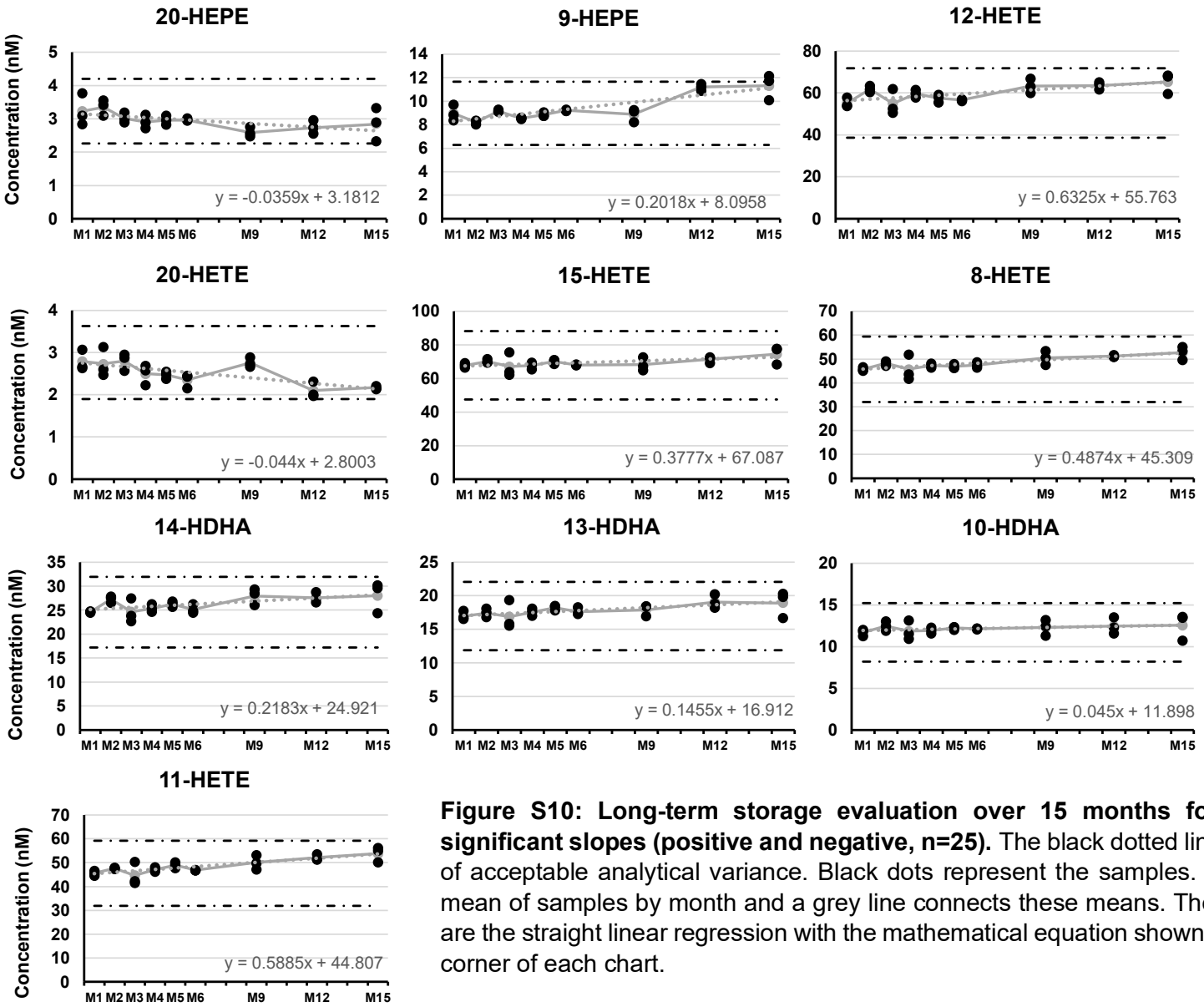

Figure S10: Long-term storage evaluation over 15 months for oxylipins with significant slopes (positive and negative, n=25). The black dotted lines mark the ±30% of acceptable analytical variance. Black dots represent the samples. Grey dots are the mean of samples by month and a grey line connects these means. The grey dotted lines are the straight linear regression with the mathematical equation shown in the bottom right corner of each chart.

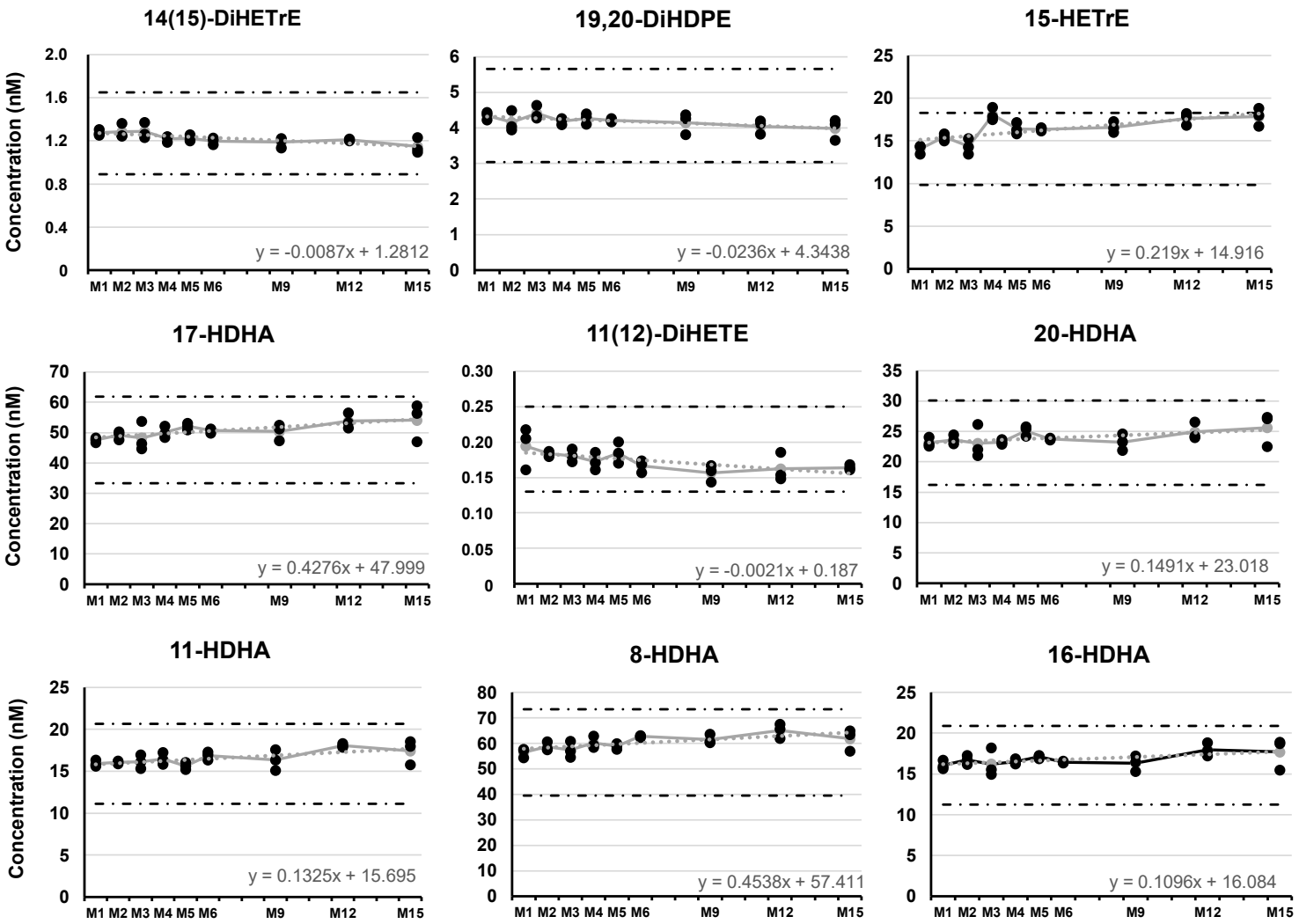

Figure S10: Continued.